Journal of Medicinal Chemistry

Article

Mathematical and Structural Characterization of Strong Non-additive SAR Caused by Protein Conformational Changes

Laurent Gomez, Rui Xu, William Sinko, Brandon Selfridge, William Francois Vernier, Kiev Ly, Richard Truong, MArkus Metz, Tami Marrone, Kristen Sebring, Yingzhuo Yan, brent appleton, Kathleen Aertgeerts, eben massari, and James Guy Breitenbucher

J. Med. Chem., **Just Accepted Manuscript** • DOI: 10.1021/acs.jmedchem.8b00713 • Publication Date (Web): 02 Aug 2018

Mathematical and Structural Characterization of Strong Non-additive SAR Caused by Protein Conformational Changes

Laurent Gomez,* Rui Xu, William Sinko, Brandon Selfridge, William Vernier, Kiev Ly, Richard Truong, Markus Metz, Tami Marrone, Kristen Sebring, Yingzhou Yan, Brent Appleton, Kathleen Aertgeerts, Mark Eben Massari, J. Guy Breitenbucher.

Dart Neuroscience LLC, 12278 Scripps Summit Drive, San Diego, CA 92131, USA

ABSTRACT: In medicinal chemistry, accurate prediction of additivity-based SAR analysis rests on three assumptions: (1) a consistent binding pose of the central scaffold, (2) no interaction between the R group substituents, and (3) a relatively rigid binding pocket in which the R group substituents act independently. Previously, example of non-additive SAR have been documented in systems that deviate from the first two assumptions. Local protein structural change upon ligand binding, through induced fit or conformational selection, although a well-known phenomenon that invalidates the third assumption, has not been linked to non-additive SAR conclusively. Here, for the first time, we present clear structural evidence that the formation of a hydrophobic pocket upon ligand binding in PDE2 catalytic site reduces the size of another distinct sub-pocket, and contributes to strong non-additive SAR between two otherwise distant R groups.

INTRODUCTION

Rational small molecule drug discovery is based on the underlying assumption that the biological properties of a molecule can be predictably altered by incorporating specific structural modifications to that molecule (Structure Activity Relationships, SAR). The process of lead optimization relies on a level of intuitive pattern recognition by the chemist in the form of SAR. Given the significance of identifying predictable SAR patterns, it was inevitable that chemists would attempt to improve their intuition by mathematically quantifying the relationship between structure and biological effect (QSAR). One of the first proposed quantitative models to exploit the additivity of SAR relationships was published in 1964 by Free and Wilson, a model now referred to as Free-Wilson Additivity.[1] Although the Free-Wilson model of additivity was quite a simple mathematical concept, the idea has had far reaching implications in drug discovery. Today the medicinal chemistry literature is dominated by papers which optimize one R group, followed by a second R group sequentially (Linear Analoging) rather than creating a matrix of compounds altering multiple R groups simultaneously (Combinatorial Analoging). When chemists engage in linear analoging they make the implicit assumption of additivity articulated in Free and Wilson's original work (i.e. the best R^1 is the best regardless of the nature of R^2). Additionally, this assumption underlies many chemical and physical descriptors that are calculated to correlate a compound's calculated physical properties and biological effect (MW is innately additive; most methods of calculating tPSA and cLogP also rely on the assumption of additivity).[2] In fact, the value of nearly all QSAR models which seek to mathematically correlate a molecule's calculated physical properties with a biological effect would be greatly compromised if the system being studied was found to be inconsistent with classical Free-Wilson additivity.[3]

Furthermore, most if not all computational scoring functions[4] including Free Energy Perturbation Methods such as FEP+ [5], work best under the conditions of additivity. However, challenges such as binding mode changes of the ligand and binding site changes are currently being actively investigated.[6-7]

In 2006 we described a method in which the Free-Wilson additivity of a combinatorial matrix could be used to evaluate structure activity relationships.[8-9] The method we developed allowed one to determine the overall Free-Wilson additivity within a combinatorial matrix of compounds. In cases where non-additivity was verified, we reasonably hypothesized that this indicated a change in binding mode between the ligands and the target protein, or suggested an interaction between the varied substituents within the set of ligands. Although this hypothesis was intuitive, we had no structural confirmation that non-additive behavior actually resulted in observable binding mode changes. In fact, although a fundamental change in binding mode is often cited as the cause of non-additive behavior in medicinal chemistry papers, there are actually very few examples where this is rigorously confirmed with structural data.[10]

In 2008 researchers from Janssen published an article whereby they used a similar method to quantify the additivity intrinsic to small molecule interactions with a variety of biological targets. The authors came to the conclusion that some targets were prone to display non-additive SAR while others were more generally additive in their interactions.[4] However, this work did not contain any structural data that could have provided useful rational and understanding for specific observed non-additive behavior.

With increased knowledge such as available ligand SAR and structural data about the target in question non-additive behavior can be studied, and in several cases it was explained by alternative intra-molecular substituent interactions or switched binding modes. [11-12]

Recently, Kramer and coworkers published a very clever procedure for determining non-additive SAR. They applied this method to publicly available SAR data.[13] In this work Kramer was able to explain non-additive data in terms of changes in ligand binding modes within the ligand-protein crystal structures in a few cases. In none of the 15 cases analyzed did the non-additivity described involve a significant induced conformational change in the protein's structure. Given the large number of examples of non-additive behavior described in the medicinal chemistry literature, we suggest that a medicinal chemistry project should never be attempted without first quantifying the degree of non-additivity intrinsic to the particular system being studied. Here we employ Kramer's method as means of quantitating the degree of non-additivity for any set of compounds using PDE2 as a specific example system. We also demonstrate how obtaining crystal structure of ligands bound the PDE2 enzyme lead to the identification of putative protein conformational changes responsible for the non-additive effects seen.

RESULTS AND DISCUSSION

In this current work we demonstrate convincingly through the use of quantitative additivity analysis, that non-additivity was significant within the matrix studied. Computational tools and X-ray crystallography were then used to demonstrate protein conformational differences among ligand co-complexes which unambiguously explained the source of the non-additive behavior. Taking together, these findings constitute a case of non-additive SAR caused by an imposed structural requirement on the protein.

The system investigated here uses a triazoloquinozaline scaffold developed by researchers at Janssen R&D as PDE2 inhibitors.[14] Each compound was synthesized according to the synthetic route shown in Scheme 1. Condensation of alanine with 4-fluoro-3-nitrobenzoic acid **1** under basic conditions afforded the desired intermediate **2** in 60% yield. A subsequent reduction of the nitro group followed by a spontaneous intramolecular cyclization yielded tetrahydroquinoxaline **3**. The intermediate was then oxidized to the desired dihydroquinoxaline **4** using hydrogen peroxide under basic conditions. Esterification of the acid moiety was accomplished by treating compound **4** with ethanol and sulfuric acid. The corresponding dihydroquinoxaline **5** was then chlorinated under standard conditions, phosphorus oxychloride and N,N-dimethylaniline, to afford the key intermediate **6** in moderate yields (17%) after column chromatography. The first set of substitutions was introduced after condensation of five differently substituted 3-chlorobenzhydrazides with intermediate **6** to provide all six triazoloquinoxaline intermediates, **7-12**, in moderate to good yields. Saponification of the ester functionality under basic conditions followed by amide bond formation afforded the desired matrix of compounds, **19-48**, which is described in Figure 1. The design was intended to test the steric tolerance of the PDE2 active site at the variable R^1 and R^2 positions in the matrix. It should be noted that a 3D energy minimized model of the compounds suggests no possible direct interaction between R^1 and R^2 due to the rigid nature of the triazoloquinozaline scaffold (Figure 1). A crystal structure of compound 1 (R^1 = Me, R^2 = H) confirmed this observation and suggests that R^1 and R^2 fit into two distinct, non-overlapping protein pockets present in the catalytic site of PDE2 (Figure 2). The triazoloquinozaline core is sandwiched in the π-clamp formed by Phe862, Phe830 and Ile826. The amide functionality is situated above the π-clamp, positioning the R^1 group in a solvent-exposed region surrounded by lipophilic residues such as Met847. The chlorophenyl group is buried deep inside the

binding pocket, near the bound metals and orients R^2 substitutions toward a water-filled channel between bound metals and Leu770.

Scheme 1: Synthetic route

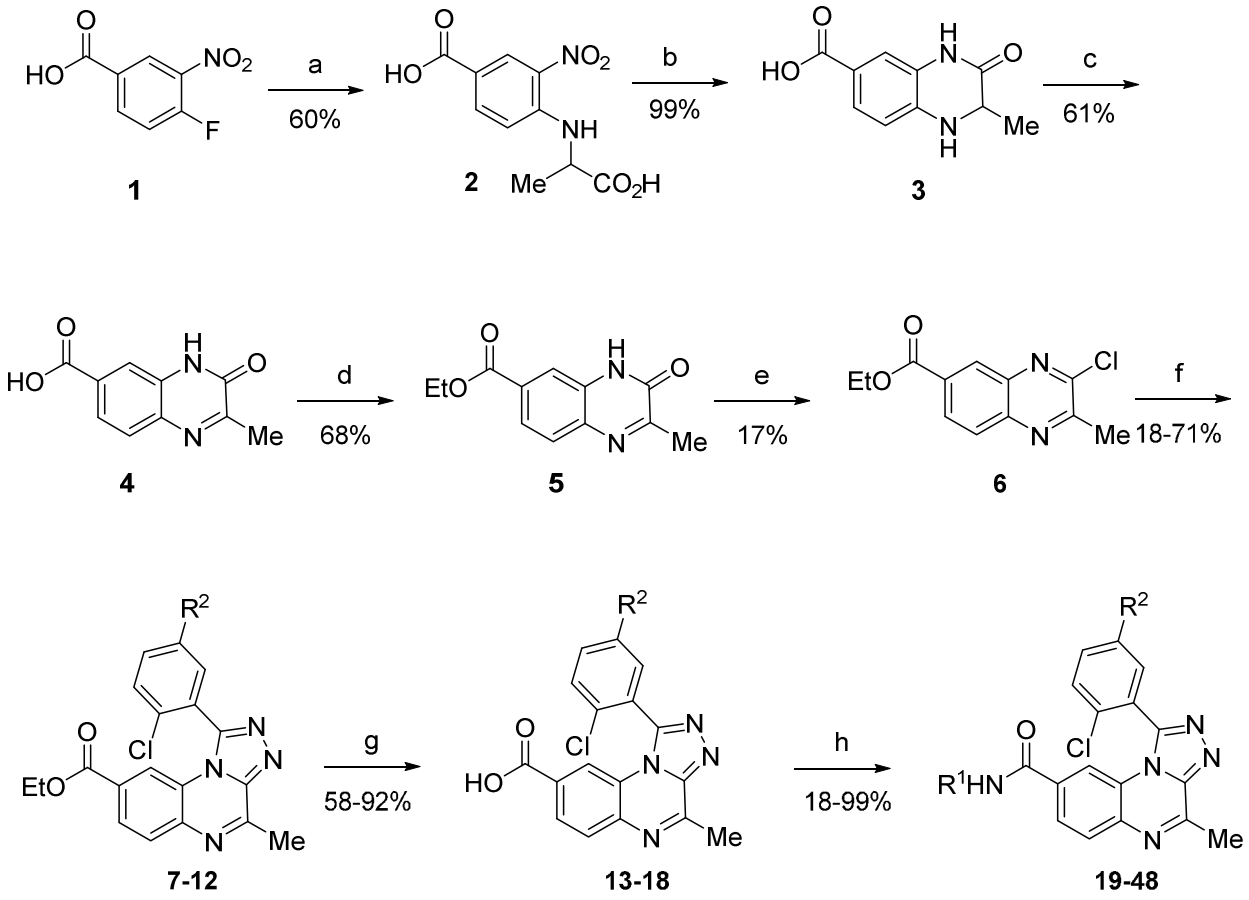

[a]Reagents and conditions: a. alanine, H_2O, $NaHCO_3$, 95 ^oC; b. Raney Ni, $NaHCO_3$, H_2O, 60 psi; c. i) 2N NaOH, 30% H_2O_2, 100 ^oC; ii) HCl; d. EtOH, H_2SO_4, 80 ^oC; e. $POCl_3$, N,N-dimethyl aniline, 120 ^oC; f. $ArCONHNH_2$, n-BuOH, 160 ^oC; g. LiOH, THF/H_2O; h) DIEA, HATU, R^1NH_2, DMF.

Figure 1: Matrix of compounds and lowest energy conformation for compound 19

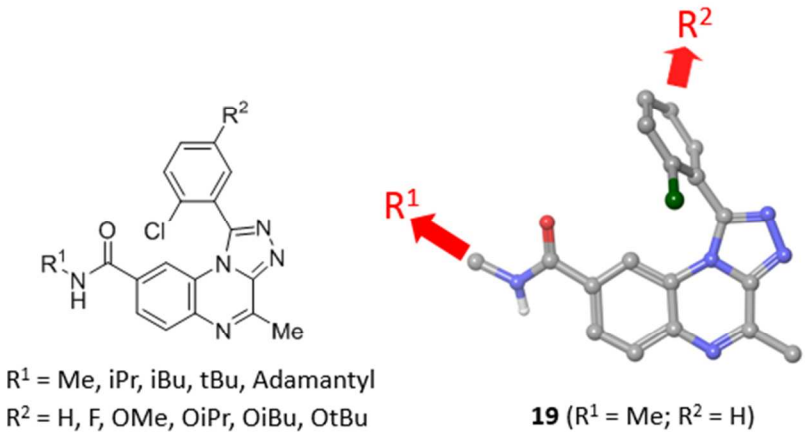

Figure 2: Crystal structure of compound 19 (PDB ID: 6C7E)

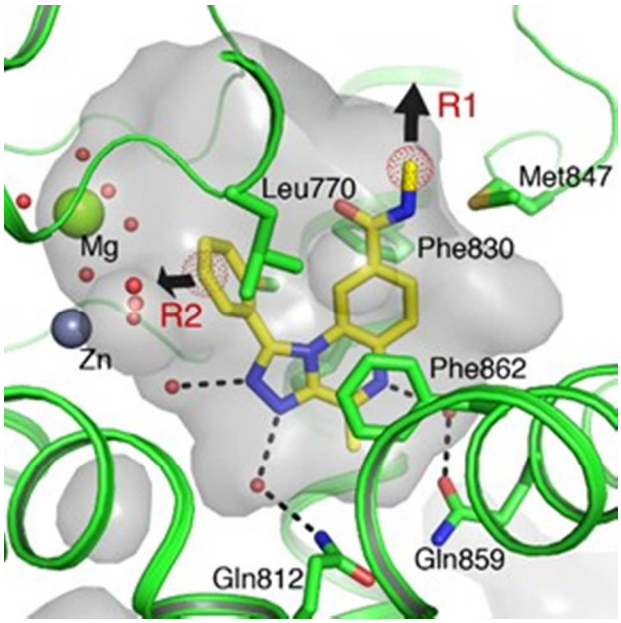

All compounds were tested for their inhibition of the PDE2 enzyme and reported as pIC_{50} and run in quadruplicate with a mean standard error of all experiments of 0.10 (Range of errors = 0.16-0.01; Table 1). We initially plotted our data in a 3D bar graph format by varying the R^1 substituent on the y-axis and the R^2 substituent on the x-axis (Figure 3). Upon analysis, this matrix represented a good data set for determining additivity due to measurable enzyme inhibition for

all compounds in the matrix, and an acceptable range of activities (pIC_{50} = 7.6-9.8; range = 2.2 log units) well above the mean standard error of the assay.

Figure 3. PDE2 pIC_{50} values of the compounds in the matrix.

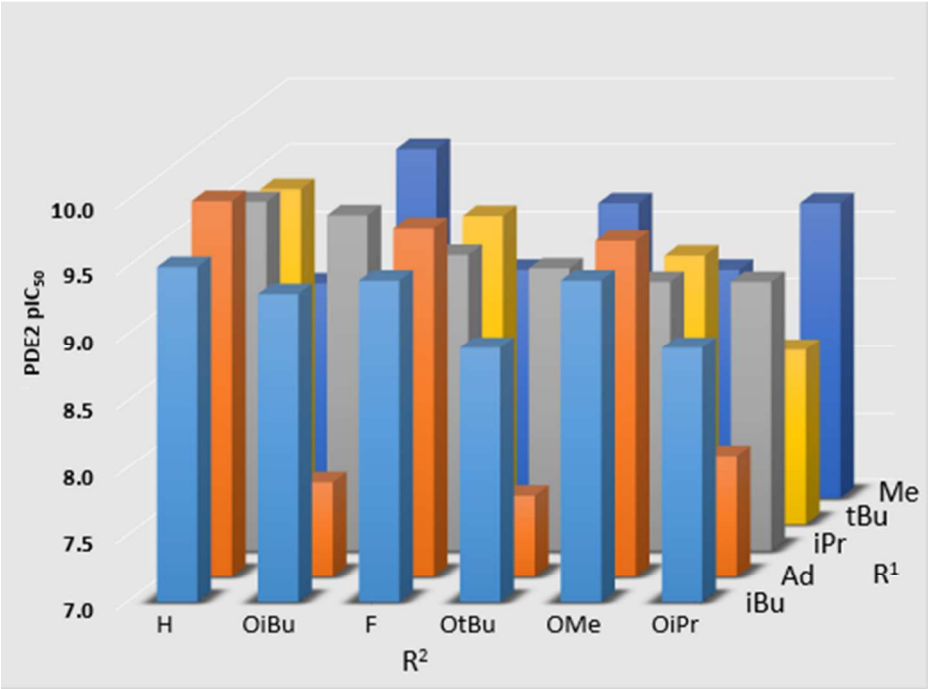

Simple visual inspection of the data depicted in Figure 3 suggests that there may be some non-additive behavior in the matrix. To quantify the degree of non-additivity we utilized the double-transformation procedure described by Kramer.[13] Using this method non-additivity can be quantified for any set of four compounds which undergo two substituent changes in two dimensions. This is illustrated in Figure 4.

Figure 4. PDE2 pIC_{50} values of selected compounds in the matrix demonstrating a lack of additivity.

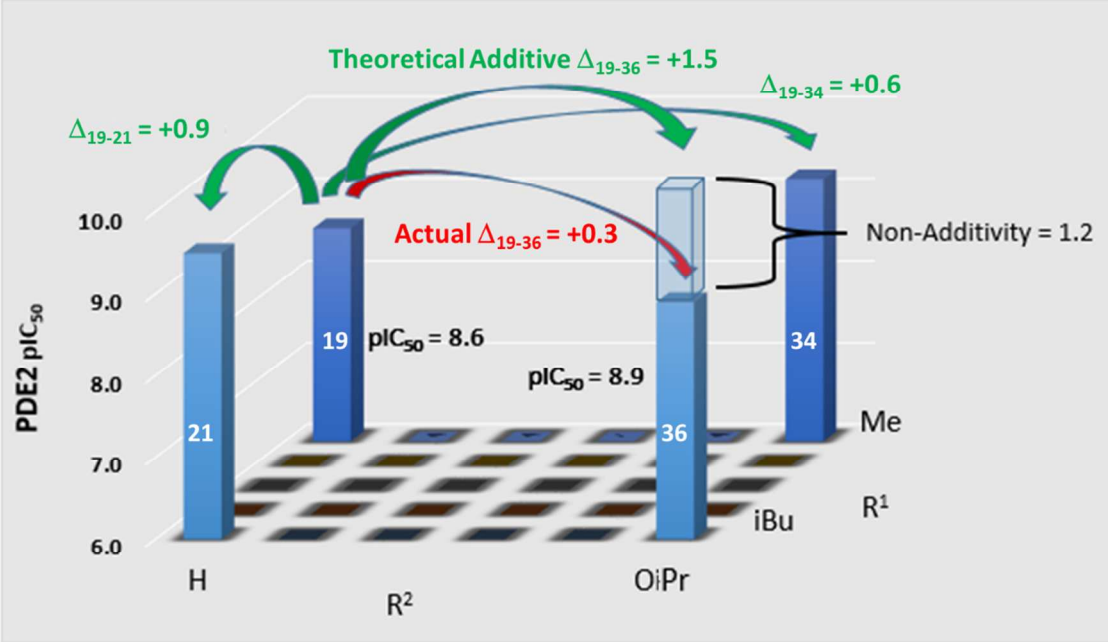

Starting with the root compound **19** in the back left (R^1 = Me, R^2 = H; pIC_{50} = 8.6) we can transform R^1 to get compound **21** (R^1 = iBu, R^2 = H; pIC_{50} = 9.5) which results in a pIC_{50} increase of 0.9. Additionally, when we transform R^2 providing compound **34** (R^1 = Me, R^2 = OiPr; pIC_{50} = 9.2) this results in a pIC_{50} increase of 0.6. However, when we perform both transformations to get compound **36** (R^1 = iBu, R^2 = OiPr; pIC_{50} = 8.9) we get a compound which is significantly less potent than we would expect if there was perfect additivity (Additive pIC_{50} = 8.6 + 0.9 + 0.6 = 10.1). Thus we quantitatively characterize this transformation as non-additive by 1.2 log units (10.1 – 8.9 = 1.2). Using the equation below allows for the quantification of non-additivity in any double-transformation of this type, as discussed by Kramer.

$$\text{non-additivity} = \text{NAd} = (pAct_3 - pAct_4) - (pAct_2 - pAct_1)$$

In order to quantify the non-additive behavior of the entire combinatorial matrix, one can use the equation above on all double-transformations. Each compound is used as starting point for 20 double-transformations considering R^1 of 5 and R^2 of 6 varied substituents. After removal of duplicate cycles 300 NAd values are produced, and their frequencies as a function of non-additivity are shown as histogram in Figure 5. As well, the experimentally observed and theoretical non-additivity distribution with a mean standard error of 0.1 are shown. All non-additivity values larger than +/- 0.52 cannot be explained with experimentally uncertainty. Thus we can determine with 99% confidence that 54% of the double transformation data contained in the current matrix is truly non-additive, and not the result of experimental uncertainty. However, we cannot judge the NAd value < 0.52 as being innately additive, there is simply too much experimental variance to make a judgement on these transformations.

Table 1. pIC_{50} data for all compounds described in the combinatorial matrix.

Compound number and pIC_{50}		R^1				
		Me	iPr	iBu	tBu	Adamantyl
R^2	H	**19** 8.55	**20** 9.57	**21** 9.52	**22** 9.47	**23** 9.77
	F	**24** 8.69	**25** 9.17	**26** 9.37	**27** 9.30	**28** 9.58
	OMe	**29** 8.74	**30** 8.96	**31** 9.42	**32** 9.00	**33** 9.49
	OiPr	**34** 9.16	**35** 8.99	**36** 8.93	**37** 8.30	**38** 7.94
	OiBu	**39**	**40**	**41**	**42**	**43**

		9.61	9.46	9.29	8.75	**7.74**
	OtBu	**44** 9.16	**45** 9.10	**46** 8.88	**47** 8.35	**48** 7.58

Figure 5. Theoretical non-additivity distribution expected from mean standard error of the assay of 0.1 log units (red line) and real non-additivity distribution (blue line). A histogram for experimental data with y axis on the right side is also shown.

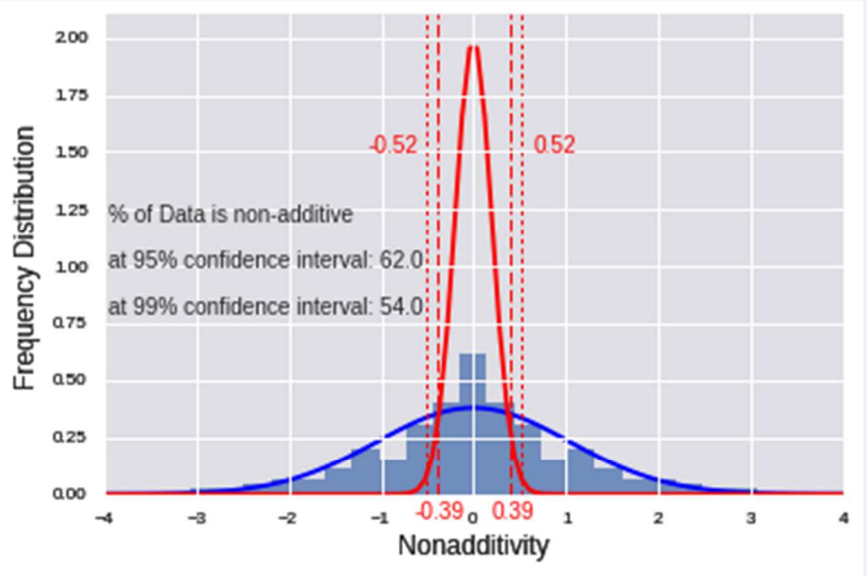

Once the non-additivity was quantitatively confirmed, we sought to understand the physical nature of the observed non-additivity within the set of compounds. Upon inspection of the double transformation data the largest non-additive value obtained in the matrix arose from the transformation; R^1 = H to OiBu, and R^2 = Me to adamantyl, resulting in an NAd = 3.1. Interestingly this represented the largest change in molecular volume within the matrix resulting in a highly significant change in expected activity. In addition, the second largest non-additive transformations also suggested that the size of the R-groups was playing a significant role in the non-additive behavior; R^1 = H to OtBu, and R^2 = Me to Ad. Because of this, we rearranged the matrix

in order of the molecular volume of the substituents and plotted the NAd calculated for each compound relative to the smallest compound in the matrix (**19**; R^1 = Me, R^2 = H) using Kramer's double transformation method (Figure 6).

Figure 6. Graphical representation of the non-additivity values for each compound relative to compound 19, the dotted line at NAd = 0.5 represents the value that provides 95% confidence that the non-additivity observed cannot be explained by the experimental uncertainty.

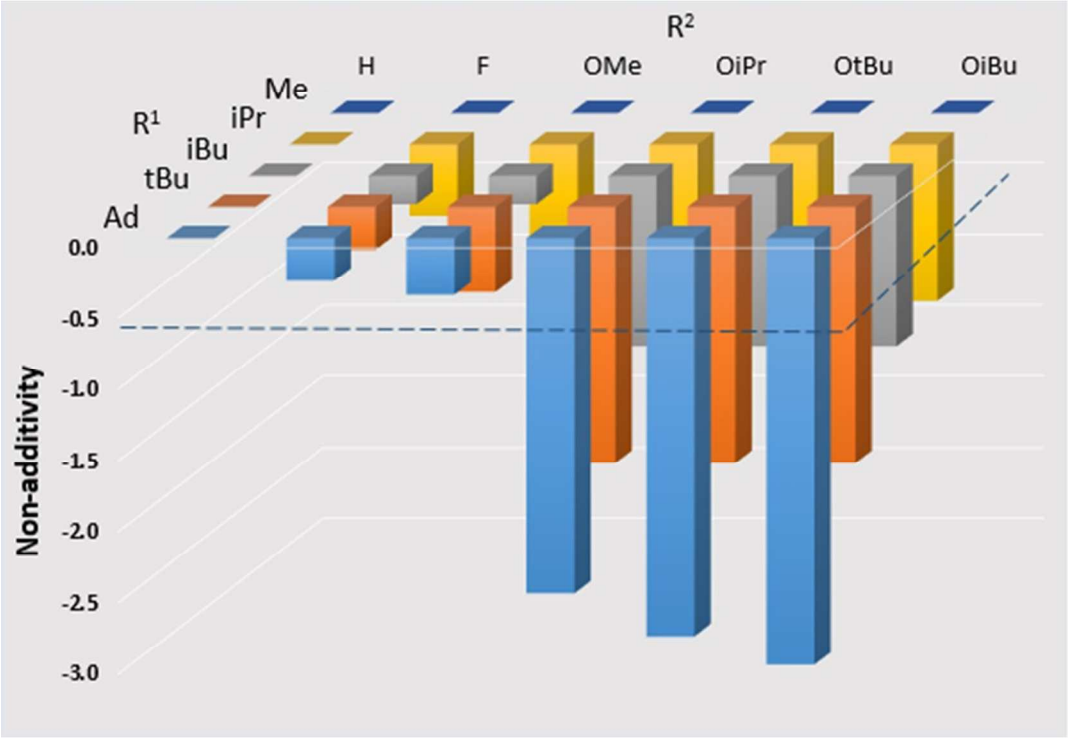

Figure 6 clearly illustrates that there is a consistent non-additive relationship within the matrix, and that the non-additivity is related to the size of the variable groups in the matrix. Seemingly, one can increase the size of each of the R-groups independently and increase the activity of the compounds, but if the size of both groups are increased together a drop in activity occurs.

Since a direct interaction between R^1 and R^2 substituents is unlikely to be the source of the non-additive behavior as we discussed previously, we decided to rely on crystallographic methods to investigate the cause of this observed phenomenon. Therefore, we selected six candidates with varying sizes of R^1 and R^2, including all four compounds presented in Figure 4 for structural determination in the co-complex of PDE2 enzyme (see supporting information). The results indicate that all six compounds adopt a similar binding mode (RMSD values ≤ 1Å; see supporting information) and rule out the possibility of ligand rearrangement in the binding site which has traditionally been a common explanation for non-additivity. Analyses of our crystal structures indicate that both R^1 and R^2 pockets can independently accommodate large hydrophobic functional groups. For example, the adamantyl group which is the largest R^1 in our tested matrix fits in the R^1 pocket and is surrounded by Leu770, Met847 and other hydrophobic residues at the entrance of the catalytic site (see supporting information). These favorable interactions contribute to about 16-fold improvement for PDE2 when compared to analog **19** and **23** (R^1 = Me and Ad respectively with R^2 = H, NAd = 1.2). More importantly and unlike the R^1 pocket, significant conformational changes are necessary to accommodate large R^2 groups.

In ligand co-complexes where a large R^2 group is presented to this part of the PDE2 enzyme, protein rearrangement is observed which primarily involves the shift of Leu770 residue and open a hydrophobic pocket near the bound metals. For example the compound with the largest R^2 group of the matrix (**39**; R^1 = Me and R^2 = OiBu) inserts into the newly formed pocket (see supporting information) and improves PDE2 inhibition by 7.9-fold when comparing analogs **19** and **39** (R^2 = H and OiBu respectively with R^1 = Me, NAd = 0.9). Similar structural changes have previously been reported for PDE2 in complex with inhibitor BAY60-7550[15a] as well as with similar PDE2 analogs described herein.[15b]

This "leucine flip" is mostly localized in the side chain of Leu770. Similar side chain flexibility as well as larger scale conformational changes concomitant with ligand binding have been well documented[16] in the literature. Protein structural changes upon ligand binding can originate from either conformational selection of one of several pre-existing conformations or an induced fit of the protein by the ligand. [17]

Comparing the structures of compounds **23** and **39** highlights the structural basis for the observed non-additivity. Favorable binding of large R^1 and R^2 substituents requires close interaction with residue Leu770, which can adapt different side chain conformations (Figure 7). In this case, Leu770 works as a molecular divider that distributes ligand binding volume between R^1 and R^2 pockets. A large R^1 group inevitably results in a small R^2 pocket, and vice versa. For this series of compounds, size increase of both R^1 and R^2 groups leads to steric clashes around Leu770 and deviation from prediction by perfect additivity. A three-dimensional representation of the non-additive SAR as a function of R-groups total surface area is shown in Figure 8. The x and y axes represent the total surface area (tSA) for R^1 and R^2 respectively plotted against the deviation from additivity (Z axis; NAd). As can be seen, the largest analog **43** (R^1 = Ad, tSA = 312.9 Å and R^2 = OiBu, tSA = 244.9) lead to the largest NAd of 3.1. The structural determination of compound **43** reveals an isobutyl group buried in the R^2 hydrophobic pocket and a highly disordered adamantyl group in the R^1 solvent-exposed pocket that displays ambiguous electron density and therefore cannot be modelled confidently. We reasoned that this is due to the steric clash between the adamantyl group and Leu770 when the R^2 hydrophobic pocket is formed. Compound **43** shows the largest difference between the actual PDE2 pIC_{50} and that predicted by perfect additivity. Thus, the non-additivity we observed can be explained by an indirect, target-mediated interaction between the size R^1 and R^2 groups and the two pockets present in the enzyme.

Figure 7: Overlay of compounds 23 (in cyan, PDB code: 6C7D) and 39 (in orange, PDB code: 6C7F) bound to PDE2 enzyme.

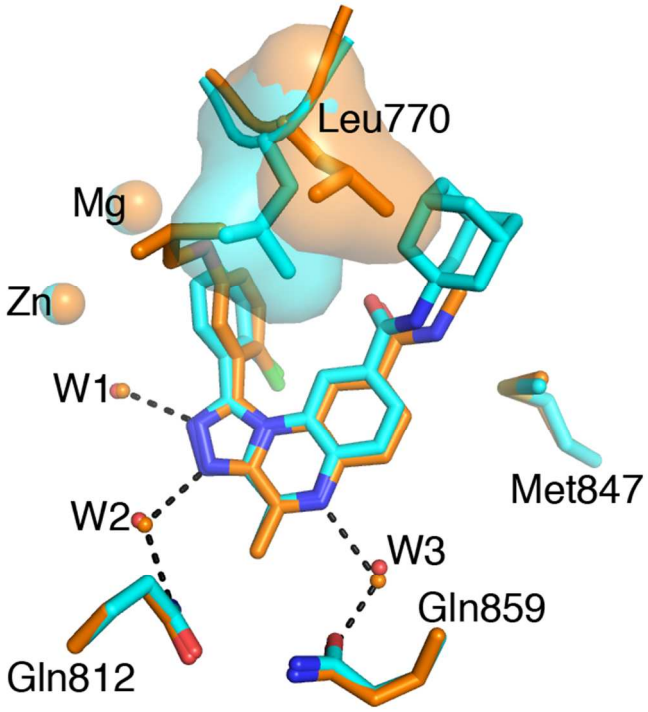

Figure 8: Correlation between R^1 and R^2 surface areas and deviation from additive SAR (NAd)

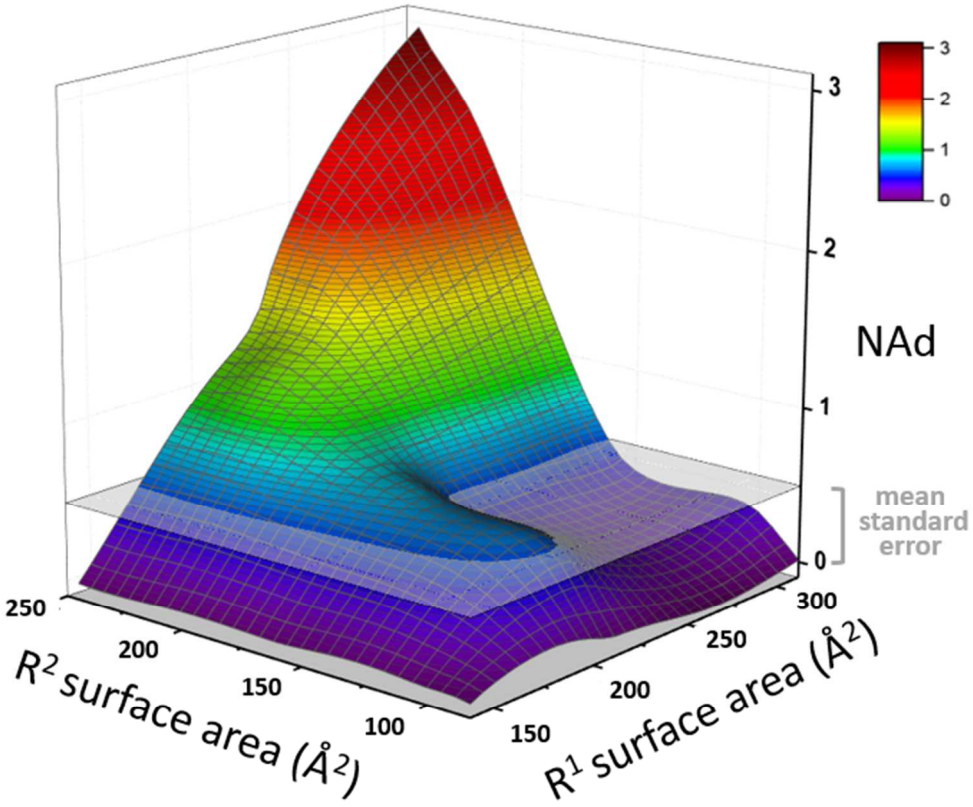

CONCLUSIONS

Given the importance and complexity of ligand-protein interactions in drug discovery, medicinal chemists continuously rely on structure activity relationships to rationally design molecules and improve their binding properties. It is therefore crucial that SAR analyses are carefully conducted in order to properly and accurately determine the optimization strategy. In this study, we have demonstrated that a process that includes a mathematical analysis of non-additivity coupled with protein-ligand co-complex structural information reveals unprecedented protein conformational change as the cause of the non-additive SAR. Our study shows that optimal inhibition of PDE2 can be achieved by balancing the size of either R^1 or R^2 substituents. Our results indicate however that the optimization of these two vectors will diverge due to non-additive SAR and therefore

no assumptions should be made. This also represents a challenge for computational scientists to predict the binding energies as conformational changes in the binding site introduce an additional source of error. In general free energy calculations seem to work better if only the ligand is modified in the binding site.

We expect that the approach and the findings discussed herein should be generally applicable to other biological targets. In effect, these results give medicinal chemists the ability to analyze and rationalize non-additive SAR which unlocks the potential of more efficiently improving ligand-protein interactions.

EXPERIMENTAL SECTION

General Methods. Solvents and reagents were purchased and used without further purification unless otherwise noted. Flash column chromatography (FCC) was performed on Teledyne Isco CombiFlash® instruments equipped with silica gel columns. Preparative HPLC purification was performed on a Waters Preparative LCMS system equipped with a Waters XBridge Prep C18 5 μm OBD 19x50 mm column. Elution was achieved with increasing concentration of acetonitrile in water and 0.05% TFA added as modifier. Analytical HPLC was performed on an Acquity UPLC system equipped with a BEH C18 1.7 μM 2.1 x 50 mm column. Elution was achieved with increasing concentration of acetonitrile in water and 0.1% formic acid added as modifier. NMR was performed on a Bruker Ultrashield 400 Plus spectrometer. Chemical shifts (δ) are reported in ppm relative to the residual solvent signal. Data for $^{1}H/^{13}C$ NMR spectra are reported as follows: chemical shift (multiplicity, coupling constants, number of hydrogens). Abbreviations are as follows: s (singlet), d (doublet), t (triplet), q (quartet), m (multiplet), br (broad).The purity

of all compounds tested was determined by LCMS and ^{1}H NMR to be >95%. High-resolution mass spectral data were obtained from the University of California, San Diego.

4-((1-Carboxyethyl)amino)-3-nitrobenzoic acid (2). To a stirring solution of 4-fluoro-3-nitrobenzoic acid (**1**; 50.0 g, 270 mmol, 1.0 eq.) in H_2O (500 mL) was added L-alanine (48 g, 540 mmol, 2.0 eq.) followed by $NaHCO_3$ (68 g, 810 mmol, 3.0 eq.). The reaction mixture was heated to 100 ^oC. After heating the reaction mixture for 36 h at 100 ^oC, the solution was cooled to room temperature and acidified with 6N HCl. The resultant precipitate was filtered and dried under vacuum to afford the title compound (**2**; 41 g, 60% yield) as a light red solid. ^{1}H NMR (300 MHz, DMSO-d_6) δ 13.16 (brs, 2H), 8.70 (d, J = 6.9 Hz, 1H), 8.64 (d, J = 1.8 Hz, 1H), 7.99 (dd, J = 9.0, 2.1 Hz, 1H), 7.09 (d, J = 9.3 Hz, 1H), 4.62–4.53 (m, 1H), 1.50 (d, J = 6.9 Hz, 3H). MS(ESI): *m/z* 255.16 $[M+H]^+$.

2-Methyl-3-oxo-3,4-dihydroquinoxaline-6-carboxylic acid (4). To a stirring solution of 4-((1-carboxyethyl)amino)-3-nitrobenzoic acid (**2**; 41.0 g, 161 mmol, 1 eq.) in H_2O (400 mL) in a bomb apparatus was added Raney Ni (30 g wet) followed by $NaHCO_3$ (40.7 g, 484 mmol, 3.0 eq.). The apparatus was evacuated and refilled with N_2 (x 2) before charging with H_2 at 60 psi. After stirring under a H_2 atmosphere at 60 psi for 60h, the reaction mixture was filtered through a pad of celite and and concentrated in vacuo to afford 2-methyl-3-oxo-3,4-dihydroquinoxaline-6-carboxylic acid (**3**; 40.0 g) crude which was carried on without further purification. MS(ESI): *m/z* 207.04 $[M+H]^+$.

The above crude (**3**; 40.0 g, 194 mmol theoretical, 1.0 eq.) was added to a stirring solution of sodium hydroxide (38.8 g, 5.0 eq.) in H_2O (400 mL) and 30% H_2O_2 solution (40 mL) at 0 °C. The reaction mixture was heated to 100 °C. After stirring at 100°C for 16h, the reaction mixture was cooled to 0 °C and acidified with 6N HCl. The precipitated solid was filtered, dried and triturated with Et_2O (40 mL) to afford the title compound (**4**; 20.0 g, 61% yield overall yield). ^{1}H NMR (300 MHz, DMSO-d_6) δ 12.46 (brs, 1H), 7.89 (s, 1H), 7.77 (brs, 2H), 3.86 (brs, 1H), 2.43 (s, 3H). MS(ESI): *m/z* 205.09 $[M+H]^+$.

Ethyl 2-methyl-3-oxo-3,4-dihydroquinoxaline-6-carboxylate (5). To a stirring solution of 2-methyl-3-oxo-3,4-dihydroquinoxaline-6-carboxylic acid (**4**; 20.0 g, 86.1 mmol, 1.0 eq.) in EtOH (400 mL) at 0 ^{o}C was added H_2SO_4 (10 mL). The reaction mixture was warmed to 80 °C. After stirring at 80 ^{o}C for 16h, the reaction mixture was cooled to room temperature, and concentrated in vacuo. The crude material was basified with $NaHCO_3$(aq.) and extracted with EtOAc (3 X 250 mL). The combined organics were dried over Na_2SO_4, filtered, and concentrated in vacuo to afford the title compound (**5**; 13.5 g, 68% yield) as a pink solid which was carried on without any further purification. ^{1}H NMR (400 MHz, DMSO-*d6*) δ 12.42 (brs, 1H), 7.89 (s, 1H), 7.78 (brs, 2H), 4.35 (q, J = 7.6 Hz, 2H), 2.43 (s, 3H), 1.34 (t, J = 7.2 Hz, 3H). MS(ESI): m/z 233.15 $[M+H]^+$.

Ethyl 3-chloro-2-methylquinoxaline-6-carboxylate (6). To a solution of ethyl 2-methyl-3-oxo-3,4-dihydroquinoxaline-6-carboxylate (**5**; 13.5 g, 58.1 mmol, 1.0 eq.) in N,N-dimethyl aniline (74 mL) was added $POCl_3$ (54.0 mL, 581 mmol, 10 eq.) dropwise. The resulting mixture was stirred at room temperature for 1 hours then heated to 120 °C. After heating the reaction mixture for 1h at 120 °C, the solution was cooled to 0 °C, diluted with $NaHSO_4$(aq.), and extracted with

EtOAc (3 X 250 mL). The combined organics were dried over Na_2SO_4, filtered, and concentrated in vacuo to obtain a crude solid. The crude solid was purified by neutral alumina gel chromatography (2% DCM in petroleum ether) to afford the title compound (**6**; 2.5 g, 17%) as an off-white solid. ^{1}H NMR (400 MHz, $CDCl_3$) δ 8.70 (d, *J* = 2.0 Hz, 1H), 8.35 (dd, *J* = 8.8, 2.0 Hz, 1H), 8.06 (d, *J* = 8.8 Hz, 1H), 4.46 (q, *J* = 6.8 Hz, 2H), 2.87 (s, 3H), 1.45 (t, *J* = 6.8 Hz, 3H). MS(ESI): *m/z* 251.04 $[M+H]^+$.

Ethyl 1-(2-chlorophenyl)-4-methyl-[1,2,4]triazolo[4,3-a]quinoxaline-8-carboxylate (7). To a stirring mixture of ethyl 3-chloro-2-methylquinoxaline-6-carboxylate (**6**; 3.0 g, 12 mmol, 1.0 eq,) in n-BuOH (45 mL) in a sealed tube was added 3-chlorobenzhydrazide (3.04 g, 17.9 mmol, 1.5 eq). The tube was sealed and heated to 160 °C. After heating at 160 °C for 3h, the reaction mixture was cooled to room temperature and diluted with EtOAc (50 mL) and H_2O (50 mL). The organic layer was separated and concentrated in vacuo to afford a crude solid. This crude mixture was purified by reversed phase HPLC (MeCN and 0.1% aqueous NH_4OAc as eluent) to afford **7** (0.800 g, 18% yield). ^{1}H NMR (300 MHz, $CDCl_3$) δ 8.21 (d, J = 8.4 Hz, 1H), 8.09 (d, J = 8.4 Hz, 1H), 7.96 (s, 1H), 7.70 (m, 3H), 7.60 (m, 1H), 4.27 (q, J = 6.9 Hz, 2H), 3.12 (s, 3H), 1.28 (s, J = 6.9 Hz, 3H). MS(ESI): m/z 367.23 $[M + H]^+$.

Ethyl 1-(2-chloro-5-fluorophenyl)-4-methyl-[1,2,4]triazolo[4,3-a]quinoxaline-8-carboxylate (8).

Preparation of 2-chloro-5-fluorobenzohydrazide (48). To a stirring solution of methyl 2-chloro-5-fluorobenzoate (1.0 g, 5.3 mmol, 1.0 eq) in EtOH (10 mL) was added hydrazine hydrate (2.8 g, 53 mmol, 10.0 eq). The reaction mixture was heated to 50 °C for 1 h. The reaction mixture was cooled to 0 °C and triturated with Et_2O (20 mL). The resultant precipitate was filtered to afford 2-chloro-5-fluorobenzohydrazide (**48**; 0.800 g, 80% yield) as white solid. ^{1}H NMR (300 MHz, DMSO-d6) δ 9.5 (brs, 1H), 7.38 (dd, *J* = 8.7, 4.8 Hz, 1H), 7.36-7.26 (m, 2H). MS(ESI): *m/z* 189.06 $[M + H]^+$.

To a stirring solution of ethyl 3-chloro-2-methylquinoxaline-6-carboxylate (**6**; 3.0 g, 12.7 mmol, 1.0 eq.) in *n*-BuOH (45 mL) in a microwave vial was added hydrazide **48** (3.1 g, 16.5 mmol, 1.3 eq.). The vial was capped and heated at 160 °C in the microwave for 1 h. After heating at 160 °C in the microwave for 1 h, the reaction mixture was cooled to room temperature and concentrated in vacuo to afford crude compound. The crude compound was purified by reverse phase column chromatography (MeCN and 0.1% aqueous NH_4OAc as eluent) to afford **6** (1.0 g, 21% yield). ^{1}H NMR (400 MHz, $CDCl_3$) δ 8.21 (dd, *J* = 8.2, 1.6 Hz, 1H), 8.11 (d, *J* = 8.8 Hz, 1H), 7.98 (d, *J* = 1.6 Hz, 1H), 7.67 (dd, *J* = 4.8, 8.8 Hz, 1H), 7.47 (m, 2H), 4.29 (q, *J* = 7.6 Hz, 2H), 3.12 (s, 3H), 1.3 (t, *J* = 7.6 Hz, 3H). MS(ESI): *m/z* 370.92 $[M + H]^+$.

Ethyl 1-(2-chloro-5-methoxyphenyl)-4-methyl-[1,2,4]triazolo[4,3-a]quinoxaline-8-carboxylate (9).

Preparation of 2-chloro-5-methoxybenzohydrazide (49). To a stirring solution of 2-chloro-5-hydroxybenzoic acid (5.0 g, 29 mmol, 1.0 eq) in DMF (50 mL) at 0 °C was added K_2CO_3 (20.0

g, 145 mmol, 5.0 eq) followed by methyl iodide (21.7 mL, 348 mmol, 12.0 eq). The reaction mixture was heated to 40 °C. After heating at 40 °C for 12 h, the reaction mixture was cooled to room temperature and diluted with pre-cooled H_2O (50 mL). The aqueous layer was extracted with ethyl acetate (3 X 50 mL). The combined organics were washed with H_2O (50 mL), dried over Na_2SO_4, filtered, and concentrated in vacuo to afford methyl 2-chloro-5-methoxybenzoate (5.2 g, 89% yield) as a liquid that was used without further purification. ^{1}H NMR (300 MHz, $CDCl_3$) δ 7.38-7.32 (m, 2H), 6.96 (dd, J = 9.0, 3.0 Hz, 1H), 3.93 (s, 3H), 3.82 (s, 3H). MS(ESI): m/z 201.19 [M + H] +. To a solution of 2-chloro-5-methoxybenzoate (5.0 g, 24.9 mmol, 1.0 eq.) in EtOH (50 mL) was added hydrazine hydrate (12.5 mL, 249 mmol, 10.0 eq). The reaction mixture was heated to 50 °C. After heating for 3 h at 50°C, the reaction mixture was cooled to 0 °C and triturated with Et_2O (100 mL). The formed precipitate was filtered to afford the title compound (**49**; 5.2 g, 84% purity by LCMS) as a white solid that was used without further purification. ^{1}H NMR (300 MHz, DMSO-d6) δ 9.58 (brs, 1H), 7.38 (d, J = 8.7 Hz, 1H), 7.01 (dd, J = 9.0, 3.3 Hz, 1H), 6.93 (d, J = 3.0 Hz, 1H), 3.77 (s, 3H). MS(ESI): m/z 201.06 $[M + H]^+$.

To a stirring solution of ethyl 3-chloro-2-methylquinoxaline-6-carboxylate (**6**; 0.75 g, 3.0 mmol, 1.0 eq) in n-BuOH (11.3 mL) in a microwave vial was added 2-chloro-5-methoxybenzohydrazide (**49**; 0.78 g, 3.9 mmol 1.3 eq). The microwave vial was capped and heated to 160 °C in the microwave. After heating at 160 °C in the microwave for 0.5 h, the reaction mixture was cooled to room temperature and concentrated in vacuo to afford crude solid. The crude compound was purified by reverse phase column chromatography (MeCN and 0.1% aqueous NH4OAc as eluent) to afford ethyl 1-(2-chloro-5-methoxyphenyl)-4-methyl-[1,2,4]triazolo[4,3-a]quinoxaline-8-carboxylate (**9**; 0.35 g, 29% yield). ^{1}H NMR (400 MHz, CDCl3) δ 8.22 (dd, J = 8.4, 1.6 Hz, 1H), 8.10 (d, J = 12.8 Hz, 1H), 8.05 (d, J = 1.6 Hz, 1H), 7.56

(dd, J = 8.0, 1.6 Hz, 1H), 7.21 (m, 2H), 4.29 (q, J = 7.6 Hz, 2H), 3.87 (s, 3H), 3.11 (s, 3H), 1.3 (t, J = 7.6 Hz, 3H). MS(ESI): m/z 397.2 $[M + H]^+$.

Ethyl 1-(2-chloro-5-isopropoxyphenyl)-4-methyl-[1,2,4]triazolo[4,3-a]quinoxaline-8-carboxylate (10).

Preparation of 2-chloro-5-isopropoxybenzohydrazide (50). To a stirring solution of 2-chloro-5-hydroxybenzoic acid (7.0 g, 41 mmol, 1.0 eq.) in DMF (70 mL) at 0 °C was added K_2CO_3 (28.0 g, 203 mmol, 5.0 eq.) and isopropyl iodide (20.3 mL, 203 mmol, 5.0 eq.). The reaction mixture was heated to 80 °C. After stirring at 80 °C for 12 h, the reaction mixture was cooled to room temperature, diluted with pre-cooled H_2O, and extracted with EtOAc (3 X 70 mL). The combined organics were washed with H_2O (70 mL), dried over Na_2SO_4, filtered, and concentrated in vacuo to afford isopropyl 2-chloro-5-isopropoxybenzoate (8.1 g, 77% yield) as a liquid that was used without further purification. ^{1}H NMR (300 MHz, $CDCl_3$) δ 7.32–7.26 (m, 2H), 6.91 (dd, *J* = 9.3, 3.3 Hz, 1H), 5.28–5.24 (m, 1H), 4.58–4.49 (m, 1H), 1.38 (d, J = 6.0 Hz, 6H), 1.33 (d, J = 6.3 Hz, 6H). MS(ESI): m/z 256.12 $[M+H]^+$. To a stirring solution of isopropyl 2-chloro-5-isopropoxybenzoate (8.0 g, 31 mmol, 1.0 eq.) in EtOH (80 mL) was added hydrazine hydrate (15.6 mL, 310 mmol, 10.0 eq.). The reaction mixture was heated to 80 °C. After heating at 80 °C for 12h, the reaction mixture was cooled to room temperature and concentrated in vacuo to obtain a crude solid. The crude solid was purified by silica gel chromatography (3% MeOH in DCM) to afford 2-chloro-5-isopropoxybenzohydrazide (**50**; 7.1 g, 100%) as an off-white solid. ^{1}H NMR (300 MHz, DMSO-d6) δ 9.52 (brs, 1H), 7.35 (d, J = 9.0 Hz, 1H), 6.98 (dd, J = 9.0, 3.0 Hz, 1H), 6.88 (d, J = 3.0 Hz, 1H), 4.66–4.58 (m, 1H), 4.45 (brs, 2H), 1.26 (d, J = 6.0 Hz, 6H). MS(ESI): m/z 229.03 [M+H]+.

To a stirring solution of ethyl 3-chloro-2-methylquinoxaline-6-carboxylate (**6**; 0.75 g, 3.0 mmol, 1.0 eq) in n-BuOH (11.3 mL) in a microwave vial was added 2-chloro-5-isopropoxybenzohydrazide (50; 0.89 g, 3.9 mmol, 1.3 eq). The vial was capped and the reaction mixture was heated to 160 °C in the microwave. After heating for 30 min at 160 °C in the microwave, the reaction mixture was cooled to room temperature and concentrated in vacuo to obtain a crude solid. The crude solid was purified by reverse phase HPLC (Reveleris C-18, 80% MeCN in 0.1% NH4OAc) to afford the title compound (**10**; 0.50 g, 39% yield) as an off-white solid. ^{1}H NMR (300 MHz, DMSO-d6) δ 8.15 (m, 2H), 7.85 (brs, 1H), 7.73 (d, J = 8.4 Hz, 1H), 7.41–7.35 (m, 2H), 4.72–4.64 (m, 1H), 4.21 (q, J = 6.6 Hz, 2H), 2.98 (s, 3H), 1.31 (d, J = 6.3 Hz, 6H), 1.24 (t, J = 6.3 Hz, 3H). MS(ESI): m/z 425.16 $[M+H]^+$.

Ethyl 1-(2-chloro-5-isobutoxyphenyl)-4-methyl-[1,2,4]triazolo[4,3-a]quinoxaline-8-carboxylate (11).

Preparation of 2-chloro-5-isobutoxybenzohydrazide (51). To a stirring solution of 2-chloro-5-hydroxybenzoic acid (7.0 g, 41 mmol, 1.0 eq.) in DMF (70 mL) at 0 °C was added K_2CO_3 (28.0 g, 203 mmol, 5.0 eq.) and 1-bromo-2-methylpropane (21.7 mL, 203 mmol, 5.0 eq.). The reaction mixture was heated to 80 °C. After heating at 80 °C for 12h, the reaction mixture was cooled to room temperature, diluted with precooled H_2O, and extracted with EtOAc (3 x 70 mL). The combined organics were washed with H_2O (70 mL), dried over Na_2SO_4, filtered, and concentrated in vacuo to afford isobutyl 2-chloro-5-isobutoxybenzoate (10.0 g, 35.1 mmol) as a liquid that was used without further purification. ^{1}H NMR (400 MHz, CDCl3) δ 7.33 (s, 1H), 7.31 (d, J = 6.0 Hz, 1H), 6.94 (dd, J = 8.8, 3.2 Hz, 1H), 4.12 (d, J = 6.4 Hz, 2H), 3.72 (d, J = 6.8 Hz, 2H), 2.11 – 2.06 (m, 2H), 1.03 (d, J = 2.4 Hz, 6H), 1.02 (d, J = 2.4 Hz, 6H). To a stirring solution

of isobutyl 2-chloro-5-isobutoxybenzoate (10.0 g, 35.1 mmol, 1.0 eq.) in EtOH (100 mL) was added hydrazine hydrate (17.6 mL, 350 mmol, 10.0 eq). The reaction mixture was heated to 80 °C. After heating at 80 °C for 12 h, the reaction mixture was cooled to room temperature and concentrated in vacuo to obtain a crude solid. The crude solid was purified by silica gel chromatography (3% MeOH in DCM) to afford 2-chloro-5-isobutoxybenzohydrazide (**51**; 8.1 g, 95% yield) as an off-white solid. ^{1}H NMR (300 MHz, DMSO-d_6) δ 9.52 (brs, 1H), 7.36 (d, J = 9.0 Hz, 1H), 7.00 (dd, J = 9.0, 3.0 Hz, 1H), 6.91 (d, J = 3.0 Hz, 1H), 4.45 (brs, 2H), 3.75 (d, J = 6.6 Hz, 2H), 2.05–1.96 (m, 1H), 0.96 (d, J = 6.6 Hz, 6H). MS(ESI): m/z 243.08 $[M+H]^+$.

To a stirring solution of ethyl 3-chloro-2-methylquinoxaline-6-carboxylate (**6**; 0.75 g, 3.0 mmol, 1.0 eq) in n-BuOH (11.3 mL) was added 2-chloro-5-isobutoxybenzohydrazide (**51**; 0.94 g, 3.87 mmol, 1.3 eq.) in a microwave vial. The vial was capped and heated to 160 °C in the microwave. After heating at 160 °C for 30 min in the microwave, the reaction mixture was cooled to room temperature and concentrated in vacuo to obtain a crude solid. The crude solid was purified by reversed phase chromatography (Reveleris C-18, 80% MeCN in 0.1% NH_4OAc(aq.)) to afford ethyl 1-(2-chloro-5-isobutoxyphenyl)-4-methyl-[1,2,4]triazolo[4,3-a]quinoxaline-8-carboxylate (**11**; 0.55 g, 42% yield) as an off-white solid. ^{1}H NMR (400 MHz, DMSO-d_6) δ 8.15–8.14 (m, 2H), 7.85 (brs, 1H), 7.74 (d, J = 8.8 Hz, 1H), 7.43–7.39 (m, 2H), 4.21 (q, J = 7.2 Hz, 2H), 3.82 (t, J = 6.4 Hz, 2H), 2.98 (s, 3H), 2.05–2.02 (m, 1H), 1.22 (t, J = 6.8 Hz, 3H), 0.97 (dd, J = 6.4, 2.8 Hz, 6H). MS(ESI): m/z 438.8 $[M+H]^+$.

Ethyl 1-(5-(tert-butoxy)-2-chlorophenyl)-4-methyl-[1,2,4]triazolo[4,3-a]quinoxaline-8-carboxylate (12).

Preparation of 5-(tert-butoxy)-2-chlorobenzohydrazide (52). To a stirred solution of methyl 2-chloro-5-hydroxybenzoate (5.0 g, 26.8 mmol, 1.0 eq) in toluene (50 mL) was added N,N-dimethylformamide di-tert-butyl acetal (12.8 mL, 53.6 mmol, 2.0 eq). The reaction mixture was heated to 110 °C. After heating at 110 °C for 16 h, the reaction mixture was cooled to room temperature and additional N,N-dimethylformamide di-tert-butyl acetal (6.4 mL, 26.8 mmol, 1.0 eq) was added. The reaction mixture was heated back to 110 °C. After heating an additional 16h at 110°C, the reaction was cooled to room temperature, and concentrated in vacuo to obtain a crude solid. The crude solid was purified by silica gel chromatography (10% EtOAc in hexanes) to afford methyl 5-(tert-butoxy)-2-chlorobenzoate (2.2 g, 34% yield) as a colorless liquid and recovered starting material (2.5 g, 50%). ^{1}H NMR (300 MHz, DMSO-d_6) δ 7.47 (d, J = 8.7 Hz, 1H), 7.35 (d, J = 2.7 Hz, 1H), 7.20 (dd, J = 9.0, 3.0 Hz, 1H), 3.85 (s, 3H), 1.31 (s, 9H). MS(ESI): m/z 243.10 $[M+H]^+$. To a stirring solution of methyl 5-(tert-butoxy)-2-chlorobenzoate (3.30 g, 13.6 mmol, 1.0 eq.) in EtOH (66 mL) was added hydrazine hydrate (11.3 mL, 136 mmol, 10.0 eq). The reaction mixture was heated to 80 °C. After heating at 80 °C for 16 h, the reaction mixture was cooled to room temperature and concentrated in vacuo to obtain crude solid. The crude solid was purified by silica gel chromatography (3% EtOH in EtOAc) to afford the title compound (**52**; 2.4 g, 73% yield) as an off-white solid. ^{1}H NMR (400 MHz, DMSO-d_6) δ 9.54 (brs, 1H), 7.37 (d, J = 8.4 Hz, 1H), 7.04 (dd, J = 8.8, 3.2 Hz, 1H), 6.93 (d, J = 2.8 Hz, 1H), 4.47 (brs, 2H), 1.30 (s, 9H). MS(ESI): m/z 243.12 $[M+H]^+$.

To a stirring solution of ethyl 3-chloro-2-methylquinoxaline-6-carboxylate (**6**; 0.12 g, 0.48 mmol, 1.0 eq.) in 2,6-lutidine (0.6 mL) was added 5-(tert-butoxy)-2-chlorobenzohydrazide (**52**; 0.12 g, 0.48 mmol, 1.0 eq.) The reaction mixture was concentrated in vacuo to afford a crude solid. The crude solid was purified by silica gel chromatography (30% EtOAc in heptanes) to

afford the title compound (**12**; 0.15 g, 71% yield). ^{1}H NMR (400MHz, $CDCl_3$) δ 8.28 (dd, J = 1.6, 8.4 Hz, 1H), 8.17 (d, J = 8.4 Hz, 1H), 8.05 - 7.99 (m, 1H), 7.63 - 7.56 (m, 1H), 7.38 - 7.31 (m, 2H), 3.16 (s, 3H), 1.43 (s, 9H). ^{13}C NMR (101MHz, $CDCl_3$) δ 168.8, 155.6, 155.1, 147.4, 144.7, 139.5, 130.8, 130.1, 129.1, 128.8, 128.7, 127.6,127.4, 125.4, 117.5, 80.3, 29.7, 28.8, 21.5. MS(ESI): m/z 410.9 $[M+H]^+$.

1-(2-Chlorophenyl)-4-methyl-[1,2,4]triazolo[4,3-a]quinoxaline-8-carboxylic acid (13). To a stirring solution of ethyl 1-(2-chlorophenyl)-4-methyl-[1,2,4]triazolo[4,3-a]quinoxaline-8-carboxylate (0.600 g, 1.77 mmol) in THF/H_2O (2:1, 16.5 mL) at 0 ^{o}C was added LiOH (0.064 g, 2.7 mmol, 1.5 eq.). The reaction mixture was warmed to room temperature. After stirring 2h, the organics were concentrated in vacuo and the remaining aqueous layer was acidified with $KHSO_4$. The aqueous layer was extracted with 5% MeOH in DCM (3 x 20 mL), dried over Na_2SO_4, filtered, and concentrated in vacuo to afford crude solid. The crude solid was triturated with Et_2O (6 mL) to afford the title compound (**13**; 0.500 g, 84% yield). ^{1}H NMR (400 MHz, DMSO-d_6): δ 13.20 (brs, 1H), 8.12 (s, 2H), 7.83 (m, 3H), 7.78 (s, 1H), 7.71 (dt, J = 11.6, 2.0 Hz, 1H), 2.98 (s, 3H). ^{13}C NMR (101 MHz, DMSO-d_6) δ 166.1, 155.0, 147.4, 144.8, 138.9, 134.1, 133.9, 133.3, 130.8, 130.5, 130.2, 128.8, 128.4,127.8, 125.6, 116.8, 21.4. EI-HR calcd for $C_{17}H_{12}ClN_4O_2$ (M^+) 339.0643, found 339.0642.

1-(2-Chloro-5-fluorophenyl)-4-methyl-[1,2,4]triazolo[4,3-a]quinoxaline-8-carboxylic acid (14). To a stirring solution of ethyl 1-(2-chloro-5-fluorophenyl)-4-methyl-[1,2,4]triazolo[4,3-a]quinoxaline-8-carboxylate (1.8 g, 4.9 mmol) in THF/H_2O (2:1, 49 mL) was added LiOH (0.30 g, 7.4 mmol, 1.5 eq.). After 3h, the organics were concentrated in vacuo. The resultant aqueous

layer was acidified with $NaHSO_4$, extracted with EtOAc, dried over Na_2SO_4, filtered, and concentrated in vacuo to afford crude compound. The crude compound was triturated with Et_2O (16 mL) to afford the title compound (**14**; 1.6 g, 92% yield) as a white solid. ^{1}H NMR (400 MHz, DMSO-*d6*) δ 13.20 (brs, 1H), 8.15 (s, 2H), 7.94 (dd, J = 9.2, 4.8 Hz, 1H), 7.84-7.83 (m, 3H), 2.99 (s, 3H). ^{13}C NMR (101 MHz, DMSO-d_6) δ 166.1, 162.81 - 159.73 (m, 1C), 155.0, 146.3 (d, J = 1.5 Hz, 1C), 144.8, 138.8, 132.6 (d, J = 8.8 Hz, 1C),130.9, 130.3, 129.9 (d, J = 3.7 Hz, 1C), 129.4 (d, J = 9.5 Hz, 1C), 128.5, 125.4, 121.28 - 120.76 (m, 1C), 120.67 - 120.22 (m, 1C), 116.7, 21.4. EI-HR calcd for $C_{17}H_{11}ClFN_4O_2$ (M^+) 357.0549, found 357.0548.

1-(2-chloro-5-methoxyphenyl)-4-methyl-[1,2,4]triazolo[4,3-a]quinoxaline-8-carboxylic acid (15). To a stirring solution of ethyl 1-(2-chloro-5-methoxyphenyl)-4-methyl-[1,2,4]triazolo[4,3-a]quinoxaline-8-carboxylate (**9**; 1.3 g, 3.3 mmol, 1.0 eq.) in THF-H_2O (2:1, 36 mL) was added LiOH (0.21 g, 4.9 mmol, 1.5 eq.). After stirring at room temperature for 3h, the organics were concentrated in vacuo. The aqueous layer was acidified with $NaHSO_4$, extracted with EtOAc, dried over Na_2SO_4, filtered, and concentrated in vacuo to afford the crude solid. This crude mixture was triturated with Et_2O (5 mL) to afford the title compound (**15**; 0.71 g, 58% yield) as a white solid. ^{1}H NMR (400 MHz, DMSO-d6) δ 13.2 (brs, 1H), 8.13 (d, J = 0.8 Hz, 2H), 7.86 (s, 1H), 7.74 (d, J = 8.8 Hz, 1H), 7.42 (m, 2H), 3.83 (s, 3H), 2.97 (s, 3H). ^{13}C NMR (101 MHz, DMSO-d6) δ 166.1, 159.1, 155.0, 147.3, 144.7, 138.8, 131.5, 130.8, 130.1, 128.4, 128.4, 125.5, 125.2, 119.6, 118.3, 117.0, 56.5, 21.4. EI-HR calcd for $C_{18}H_{14}ClN_4O_3$ (M^+) 369.0749, found 369.0749.

1-(2-Chloro-5-isopropoxyphenyl)-4-methyl-[1,2,4]triazolo[4,3-a]quinoxaline-8-carboxylic acid (16). To a stirring solution of ethyl 1-(2-chloro-5-isopropoxyphenyl)-4-methyl-[1,2,4]triazolo[4,3-a]quinoxaline-8-carboxylate (**10**; 3.0 g, 7.1 mmol, 1.0 eq) in 1:1 mixture of

THF/H_2O (120 mL) was added lithium hydroxide (0.42 g, 18 mmol, 2.5 eq.). After stirring for 4 h, the reaction mixture was concentrated in vacuo to obtain a crude solid. The crude solid was dissolved in H_2O (40 mL) and washed with EtOAc (3 x 40 mL). The aqueous layer was acidified with $NaHSO_4$ (aq.) and extracted with EtOAc (3 x 40 mL). The combined organic layers were dried over Na_2SO_4, filtered and concentrated in vacuo to afford the title compound (**16**; 2.15 g, 76% yield). ^{1}H NMR (400 MHz, DMSO-d_6) δ 13.21 (brs, 1H), 8.12 (d, J = 0.8 Hz, 2H), 7.85 (brs, 1H), 7.71 (d, J = 8.8 Hz, 1H), 7.40 (d, J = 3.2 Hz, 1H), 7.36 (dd, J = 8.8, 3.2 Hz, 1H), 4.68 (m, 1H), 2.98 (s, 3H), 1.28 (dd, J = 14.8, 6.0 Hz, 6H). ^{13}C NMR (101 MHz, DMSO-d6) δ 166.1, 157.3, 154.9, 147.2, 144.7, 138.8, 131.6, 130.9, 130.1, 128.5, 128.4, 125.6, 124.8, 121.2, 119.9, 117.0, 70.9, 22.0, 21.9, 21.4. EI-HR calcd for $C_{20}H_{18}ClN_4O_3$ (M^+) 397.1062, found 397.1061.

1-(2-Chloro-5-isobutoxyphenyl)-4-methyl-[1,2,4]triazolo[4,3-a]quinoxaline-8-carboxylic acid (17). To a stirring solution of ethyl 1-(2-chloro-5-isobutoxyphenyl)-4-methyl-[1,2,4]triazolo[4,3-a]quinoxaline-8-carboxylate (**11**; 2.35 g, 5.35 mmol, 1.0 eq) in 1:1 mixture of THF/H_2O (94 mL) was added lithium hydroxide (0.32 g, 13 mmol, 2.5 eq). After stirring for 3h, the reaction mixture was concentrated in vacuo to obtain a crude solid. The crude solid was dissolved in H2O (35 mL) and washed with EtOAc (3 x 35 mL). The aqueous layer was acidified with NaHSO4 (aq.) and extracted with EtOAc (3 x 40 mL). The combined organic layers were dried over Na2SO4, filtered and concentrated in vacuo to afford the title compound (**17**; 1.73 g, 79% yield). ^{1}H NMR (300 MHz, DMSO-d6) δ 13.21 (brs, 1H), 8.13 (d, J = 0.9 Hz, 2H), 7.87 (brs, 1H), 7.72 (d, J = 9.0 Hz, 1H), 7.42–7.36 (m, 2H), 3.85–3.80 (m, 2H), 2.98 (s, 3H), 2.06–1.99 (m, 1H), 0.96 (dd, J = 6.9, 3.3 Hz, 6H). ^{13}C NMR (101 MHz, DMSO-d_6) δ 166.1, 158.6,

155.0, 147.3, 144.7, 138.9, 131.5, 130.8, 130.1, 128.4, 128.4, 125.6,125.0, 120.2, 118.8, 117.0, 75.0, 28.0, 21.4, 19.4. EI-HR calcd for $C_{21}H_{20}ClN_4O_3$ (M^+) 411.1218, found 411.1215.

1-(5-(tert-Butoxy)-2-chlorophenyl)-4-methyl-[1,2,4]triazolo[4,3-a]quinoxaline-8-carboxylic acid (18). To a stirring solution of ethyl 1-(5-(tert-butoxy)-2-chlorophenyl)-4-methyl-[1,2,4]triazolo[4,3-a]quinoxaline-8-carboxylate (**12**; 0.80 g, 1.8 mmol, 1.0 eq) in THF (8 mL) was added 1M LiOH(aq.) (0.32 g, 8.0 mmol, 4.4 eq). The reaction mixture was heated to 50 °C. After heating at 50 °C for 2h, the reaction mixture was cooled to room temperature and diluted with H_2O (25 mL). The pH was adjusted to 5 with 1N HCl and extracted with DCM (2 x 25 mL). The combined organics were dried over Na_2SO_4, filtered and concentrated in vacuo to afford the title compound (**18**; 0.60 g, 80% yield) as a light-yellow solid that was used without further purification. ^{1}H NMR (400 MHz, $CDCl_3$) δ 10.10 – 9.25 (m, 1 H), 8.34 - 8.24 (m, 1 H), 8.19 (m, 1 H), 8.06 – 7.99 (m, 1 H), 7.63 - 7.55 (m, 1 H), 7.35 - 7.30 (m, 2 H), 3.25 - 3.07 (m, 3 H), 1.41 (s, 9 H). ^{13}C NMR (101 MHz, $CDCl_3$) δ 168.8, 155.6, 155.1, 147.4, 144.7, 139.5, 130.8, 130.1, 129.1, 128.8, 128.7, 127.6, 127.4, 125.4, 117.5, 80.3, 29.7, 28.8, 21.5. EI-HR calcd for $C_{21}H_{20}ClN_4O_3$ (M^+) 411.1218, found 411.1218.

General procedure for amide coupling reaction

To a stirring solution of carboxylic acid (0.20 mmol, 1.0 eq) in DMF (1.0 mL) was added HATU (0.24 mmol, 1.2 eq.), diisopropylethylamine (0.41 mmol, 2.1 eq.), and respective amine (0.26 mmol, 1.3 eq.). After 2 h, the reaction mixture was filtered and purified by reversed phase HPLC. The resultant aqueous fractions were basified with $NaHCO_3$(aq.), extracted with DCM (3

x 20 mL), dried over Na_2SO_4, filtered, and concentrated in vacuo to afford the respective desired amide product.

1-(2-Chlorophenyl)-N,4-dimethyl-[1,2,4]triazolo[4,3-a]quinoxaline-8-carboxamide (19). Using the general procedure for amide coupling reaction with carboxylic acid **13** (70.0 mg, 0.21 mmol) afforded the title compound (**19**; 67 mg, 92% yield). Isolation by filtration without purification by reversed phase HPLC. ^{1}H NMR (400MHz, DMSO-d_6) δ 8.71 - 8.56 (m, 1H), 8.17 - 7.97 (m, 2H), 7.89 - 7.65 (m, 5H), 2.97 (s, 3H), 2.73 (d, J = 4.5 Hz, 3H). ^{13}C NMR (101MHz, DMSO-d_6) δ 165.0, 154.2, 147.4, 144.8, 137.8, 134.5, 134.2, 133.8, 133.2, 130.6, 129.7, 128.8, 127.8, 125.8, 125.6, 115.7, 40.7, 40.3, 39.8, 39.4, 26.9, 21.4. EI-HR calcd for $C_{18}H_{15}ClN_5O$ (M^+) 352.0960, found 352.0960.

1-(2-Chlorophenyl)-N-isopropyl-4-methyl-[1,2,4]triazolo[4,3-a]quinoxaline-8-carboxamide (20). Using the general procedure for amide coupling reaction with carboxylic acid **13** (80.0 mg, 0.24 mmol) and isopropylamine (40 μL, 0.47 mmol, 2.0 eq.) afforded the title compound (**20**; 43 mg, 48% yield). ^{1}H NMR (400MHz, DMSO-d_6) δ 8.31 (d, J = 7.7 Hz, 1H), 8.10 (s, 2H), 7.87 - 7.79 (m, 3H), 7.74 - 7.68 (m, 2H), 4.00 (dd, J = 6.7, 14.1 Hz, 1H), 2.97 (s, 3H), 1.11 (dd, J = 6.5, 10.1 Hz, 6H). ^{13}C NMR (101MHz, DMSO-d_6) δ 163.8, 154.1, 147.4, 144.8, 137.7, 134.9, 134.2, 133.8, 133.3, 130.5, 129.6, 128.7, 127.8, 126.0, 125.6, 115.7, 41.7, 22.7, 22.7, 21.4. EI-HR calcd for $C_{20}H_{19}ClN_5O$ (M^+) 380.1270, found 380.1273.

1-(2-Chlorophenyl)-N-isobutyl-4-methyl-[1,2,4]triazolo[4,3-a]quinoxaline-8-carboxamide (21). Using the general procedure for amide coupling with carboxylic acid **13** (70.0 mg, 0.21 mmol) and isobutylamine (27 μL, 0.27 mmol, 1.3 eq.) afforded the title compound (**21**; 83 mg, 100% yield). ^{1}H NMR (400MHz, $CDCl_3$) δ 8.02 (d, J = 8.4 Hz, 1H), 7.90 (dd, J = 1.5, 8.4 Hz,

1H), 7.73 - 7.60 (m, 4H), 7.61 - 7.49 (m, 1H), 6.31 (br. s., 1H), 3.18 (td, J = 6.5, 10.9 Hz, 2H), 3.07 (s, 3H), 1.91 - 1.68 (m, 1H), 0.90 (d, J = 6.7 Hz, 6H). ^{13}C NMR (101MHz, $CDCl_3$) δ 165.4, 154.4, 147.5, 144.8, 138.0, 135.0, 134.6, 133.1, 132.6, 130.2, 130.0, 127.9, 127.5, 125. 7, 125.5, 114.6, 77.4, 77.1, 76.8, 47.5, 28.4, 21.4, 20.2. EI-HR calcd for $C_{21}H_{21}ClN_5O$ (M^+) 394.1429, found 394.1427.

N-(tert-Butyl)-1-(2-chlorophenyl)-4-methyl-[1,2,4]triazolo[4,3-a]quinoxaline-8-carboxamide (22). Using the general procedure for amide coupling with carboxylic acid **13** (55 mg, 0.16 mmol) and tert-butylamine (22 μL, 0.21 mmol, 1.3 eq.) afforded the title compound (**22**; 32 mg, 50% yield). ^{1}H NMR (400 MHz, MeOD-d_4) δ 8.08 (d, J = 8.6 Hz, 1 H), 7.95 (dd, J = 8.6, 1.7 Hz, 1 H), 7.71 - 7.82 (m, 3 H), 7.54 - 7.71 (m, 2 H), 3.07 (s, 3 H), 1.37 (s, 9 H). ^{13}C NMR (101 MHz, MeOD-d_4) δ 166.3, 153.9, 147.7, 144.6, 137.5, 136.4,134.9, 133.3, 132.5, 130.2, 129.6, 128.0, 126.9, 126.4, 125.1, 114.7, 51.7, 28.0, 20.5. EI-HR calcd for $C_{21}H_{21}ClN_5O$ (M^+) 394.1429, found 394.1427.

N-((3s,5s,7s)-Adamantan-1-yl)-1-(2-chlorophenyl)-4-methyl-[1,2,4]triazolo[4,3-a]quinoxaline-8-carboxamide (23). Using the general procedure for amide coupling with carboxylic acid **13** (80 mg, 0.24 mmol) and adamantylamine (46 mg, 0.31 mmol, 1.3 eq.) afforded the title compound (**23**; 74 mg, 66% yield). ^{1}H NMR (400MHz, DMSO-d_6) δ 8.09 - 8.05 (m, 1H), 8.04 - 8.00 (m, 1H), 7.88 - 7.81 (m, 3H), 7.75 - 7.67 (m, 1H), 7.62 (s, 1H), 7.58 (d, J = 1.6 Hz, 1H), 2.97 (s, 3H), 2.04 (br. s., 3H), 1.96 (d, J = 2.4 Hz, 6H), 1.64 (br. s., 6H). ^{13}C NMR (101MHz, DMSO-d_6) δ 164.7, 154.0, 147.3, 144.8, 137.6, 136.2, 134.2, 133.8, 133.4, 130.5,

129.5, 128.7, 127.7, 126.6, 125.4, 115.4, 52.1, 41.2, 36.5, 29.3, 21.3. EI-HR calcd for $C_{27}H_{27}ClN_5O$ (M^+) 472.1899, found 472.1899.

1-(2-Chloro-5-fluorophenyl)-N,4-dimethyl-[1,2,4]triazolo[4,3-a]quinoxaline-8-carboxamide (24). Using the general procedure for amide coupling with carboxylic acid (**14**; 70 mg, 0.20 mmol) and methylamine (0.13 mL, 0.26 mmol, 1.3 eq.) afforded title compound (**24**; 72 mg, 99% yield). ^{1}H NMR (400MHz, DMSO-d_6) δ 8.66 (d, J = 4.0 Hz, 1H), 8.32 (s, 1H), 8.10 (d, J = 7.5 Hz, 2H), 7.97 - 7.87 (m, 1H), 7.78 (s, 3H), 2.97 (s, 3H), 2.76 (d, J = 4.2 Hz, 3H). ^{13}C NMR (101MHz, DMSO-d_6) δ 164.9, 162.5, 160.0, 154.1, 146.3, 144.8, 137.7, 134.5, 132.6, 132.5, 129.9, 129.9, 129.8, 129.5, 129.4, 125.7, 125.6, 121.1, 120.9, 120.5, 120.3, 115.7, 79.7, 40.7, 40.2, 39.8, 39.4, 26.9, 21.4. EI-HR calcd for $C_{18}H_{14}ClFN_5O$ (M^+) 370.0865, found 370.0862.

1-(2-Chloro-5-fluorophenyl)-N-isopropyl-4-methyl-[1,2,4]triazolo[4,3-a]quinoxaline-8-carboxamide (25). Using the general procedure for amide coupling with carboxylic acid (**14**; 70 mg, 0.20 mmol) and isopropylamine (22 μL, 0.26 mmol, 1.3 eq.) afforded title compound (**25**; 68 mg, 87% yield). ^{1}H NMR (400MHz, DMSO-d_6) δ 8.39 (d, J = 7.1 Hz, 1H), 8.12 (d, J = 4.4 Hz, 2H), 7.73 (br. s., 4H), 4.23 - 3.86 (m, 1H), 2.97 (br. s., 3H), 1.13 (t, J = 6.3 Hz, 6H). ^{13}C NMR (101MHz, DMSO-d_6) δ 163.7, 163.6, 162.5, 160.0, 154.1, 146.2, 144.8, 137.7, 134.9, 134.9, 132.6, 132.5, 129.9, 129.7, 129.4, 126.1, 125.4, 121.1, 120.9, 120.6, 120.4, 115.7, 41.7, 41.6, 40.7, 40.2, 39.8, 39.4, 22.7, 21.4. EI-HR calcd for $C_{20}H_{18}ClFN_5O$ (M^+) 398.1178, found 398.1177.

1-(2-Chloro-5-fluorophenyl)-N-isobutyl-4-methyl-[1,2,4]triazolo[4,3-a]quinoxaline-8-carboxamide (26). Using the general procedure for amide coupling with carboxylic acid (**14**; 70 mg, 0.20 mmol) and isobutylamine (25 μL, 0.26 mmol, 1.3 eq.) afforded title compound (**26**; 74 mg, 92% yield). ^{1}H NMR (400MHz, DMSO-d_6) δ 8.12 (br. s., 2H), 7.99 - 7.55 (m, 4H), 3.48 - 2.75 (m, 5H), 1.78 (br. s., 1H), 0.86 (br. s., 6H). ^{13}C NMR (101MHz, DMSO-d_6) δ 164.9, 164.8, 162.5, 160.0, 154.1, 146.3, 144.8, 137.7, 135.0, 135.0, 132.6, 132.5, 129.8, 129.8, 129.4, 129.4, 126.1, 125.5, 121.1, 120.9, 120.6, 120.3, 115.5, 47.3, 47.1, 40.6, 40.2, 39.8, 39.4, 28.5, 21.4, 20.6. EI-HR calcd for $C_{21}H_{20}ClFN_5O$ (M^+) 412.1335, found 412.1334.

N-(tert-Butyl)-1-(2-chloro-5-fluorophenyl)-4-methyl-[1,2,4]triazolo[4,3-a]quinoxaline-8-carboxamide (27). Using the general procedure for amide coupling with carboxylic acid (**14**; 70 mg, 0.20 mmol) and tert-butylamine (27 μL, 0.26 mmol, 1.3 eq.) afforded the title compound (**27**; 73 mg, 91% yield). ^{1}H NMR (400MHz, $CDCl_3$) δ 8.05 (d, J = 7.9 Hz, 1H), 7.88 (d, J = 7.8 Hz, 1H), 7.73 - 7.57 (m, 2H), 7.53 - 7.33 (m, 2H), 5.77 (br. s., 1H), 3.08 (br. s., 3H), 1.40 (br. s., 9H). ^{13}C NMR (101MHz, $CDCl_3$) δ 164.6, 162.4, 159.9, 154.2, 146.2, 144.8, 137.7, 135.9, 131.6, 131.5, 130.21, 130.17, 130.06, 129.2, 129.1, 125.9, 125.1, 120.3, 120.2, 120.0, 119.9, 114.0, 77.3, 77.2, 77.0, 51.9, 28.7, 21.3. EI-HR calcd for $C_{21}H_{20}ClFN_5O$ (M^+) 412.1335, found 412.1332.

N-((3s,5s,7s)-Adamantan-1-yl)-1-(2-chloro-5-fluorophenyl)-4-methyl-[1,2,4]triazolo[4,3-a]quinoxaline-8-carboxamide (28). Using the general procedure for amide coupling with carboxylic acid (**14**; 70 mg, 0.20 mmol) and adamantylamine (39 mg, 0.26 mmol, 1.3 eq.) afforded title compound (**28**; 74 mg, 77% yield). ^{1}H NMR (400MHz, DMSO-d_6) δ 8.32 (s, 1H), 8.13 -

8.02 (m, 2H), 7.93 (dd, J = 5.0, 8.9 Hz, 1H), 7.85 - 7.69 (m, 3H), 7.60 (s, 1H), 2.98 (s, 3H), 2.12 - 2.02 (m, 3H), 1.98 (br. s., 6H), 1.65 (br. s., 6H). ^{13}C NMR (101MHz, DMSO-d_6) δ 164.7, 162.5, 160.0, 153.9, 146.2, 144.8, 137.6, 136.2, 132.6, 132.5, 130.0, 129.9, 129.6, 129.5, 129.4, 126.8, 125.2, 121.1, 120.9, 120.7, 120.5, 115.5, 79.7, 52.2, 41.2, 40.7, 40.3, 39.8, 39.4, 36.5, 29.3, 21.4. EI-HR calcd for $C_{27}H_{26}ClFN_5O$ (M^+) 490.1804, found 490.1802.

1-(2-Chloro-5-methoxyphenyl)-N,4-dimethyl-[1,2,4]triazolo[4,3-a]quinoxaline-8-carboxamide (29). Using the general procedure for amide coupling reaction with carboxylic acid (**15**; 100 mg, 0.27 mmol) and methylamine (0.27 mL, 0.54 mmol, 2.0 eq.) afforded methyl amide (**29**; 33 mg, 31% yield). ^{1}H NMR (400MHz, DMSO-d_6) δ 8.63 (d, J = 4.5 Hz, 1H), 8.14 - 8.10 (m, 1H), 8.09 - 8.04 (m, 1H), 7.85 (d, J = 1.5 Hz, 1H), 7.76 - 7.69 (m, 1H), 7.43 - 7.36 (m, 2H), 3.85 (s, 3H), 2.97 (s, 3H), 2.75 (d, J = 4.5 Hz, 3H). ^{13}C NMR (101MHz, DMSO-d_6) δ 165.0, 159.0, 154.1, 147.3, 144.7, 137.7, 134.5, 131.5, 129.7, 128.5, 125.7, 125.6, 125.2, 119.5, 118.3, 115.9, 56.4, 26.9, 21.3. EI-HR calcd for $C_{19}H_{17}ClN_5O_2$ (M^+) 382.1065, found 382.1065.

1-(2-Chloro-5-methoxyphenyl)-N-isopropyl-4-methyl-[1,2,4]triazolo[4,3-a]quinoxaline-8-carboxamide (30). Using the general procedure for amide coupling with carboxylic acid (**15**; 80 mg, 0.22 mmol) and isopropylamine (17 mg, 0.28 mmol, 1.3 eq.) afforded title compound (16 mg, 18% yield). ^{1}H NMR (400MHz, DMSO-d_6) δ 8.33 (d, J = 7.7 Hz, 1H), 8.14 - 8.08 (m, 2H), 7.79 (s, 1H), 7.72 (d, J = 8.8 Hz, 1H), 7.43 - 7.41 (m, 1H), 7.40 - 7.36 (m, 1H), 4.09 - 3.96 (m, 1H), 3.85 (s, 3H), 2.97 (s, 3H), 1.12 (dd, J = 6.7, 8.2 Hz, 6H). ^{13}C NMR (101MHz, DMSO-d_6) δ 163.9, 159.0, 154.0, 147.3, 144.7, 137.7, 135.0, 131.4, 129.6, 128.5, 126.0, 125.6, 125.2, 119.5,

118.4, 115.9, 56.4, 41.7, 22.7, 22.7, 21.3. EI-HR calcd for $C_{21}H_{21}ClN_5O_2$ (M^+) 410.1378, found 410.1377.

1-(2-Chloro-5-methoxyphenyl)-N-isobutyl-4-methyl-[1,2,4]triazolo[4,3-a]quinoxaline-8-carboxamide (31). Using the general procedure for amide coupling with carboxylic acid (**15**; 80 mg, 0.22 mmol) and isobutylamine (21 mg, 0.28 mmol, 1.3 eq.) afforded the title compound (**31**; 35 mg, 38% yield). ^{1}H NMR (400MHz, DMSO-d_6) δ 8.58 (t, J = 5.7 Hz, 1H), 8.17 - 8.04 (m, 2H), 7.82 - 7.77 (m, 1H), 7.75 - 7.65 (m, 1H), 7.41 (d, J = 3.1 Hz, 1H), 7.40 - 7.35 (m, 1H), 3.84 (s, 3H), 3.11 - 2.94 (m, 5H), 1.85 - 1.72 (m, 1H), 0.85 (dd, J = 0.7, 6.7 Hz, 6H). ^{13}C NMR (101MHz, DMSO-d_6) δ 165.0, 159.0, 154.1, 147.3, 144.8, 137.7, 135.1, 131.4, 129.7, 128.5, 126.0, 125.6, 125.2, 119.5, 118.4, 115.7, 56.4, 47.2, 28.5, 21.3. EI-HR calcd for $C_{22}H_{23}ClN_5O_2$ (M^+) 424.1535, found 424.1534.

N-(tert-Butyl)-1-(2-chloro-5-methoxyphenyl)-4-methyl-[1,2,4]triazolo[4,3-a]quinoxaline-8-carboxamide (32). Using the general procedure for amide coupling with carboxylic acid (**15**; 80 mg, 0.22 mmol) and tert-butylamine (21 mg, 0.28 mmol, 1.3 eq.) afforded the title compound (**32**; 30 mg, 33% yield). ^{1}H NMR (400MHz, DMSO-d_6) δ 8.10 - 8.06 (m, 1H), 8.05 - 8.00 (m, 1H), 7.78 (s, 1H), 7.75 - 7.70 (m, 1H), 7.64 (d, J = 1.6 Hz, 1H), 7.44 - 7.42 (m, 1H), 7.41 - 7.37 (m, 1H), 3.88 - 3.83 (m, 3H), 2.97 (s, 3H), 1.30 (s, 9H). ^{13}C NMR (101MHz, DMSO-d_6) δ 165.2, 159.0, 153.9, 147.2, 144.7, 137.5, 136.2, 131.4, 129.5, 128.4, 126.7, 125.31, 125.26, 119.6, 118.4, 115.6, 56.4, 51.4, 28.8, 21.3. EI-HR calcd for $C_{22}H_{23}ClN_5O_2$ (M^+) 424.1535, found 424.1534.

N-((3s,5s,7s)-Adamantan-1-yl)-1-(2-chloro-5-methoxyphenyl)-4-methyl-[1,2,4]triazolo[4,3-a]quinoxaline-8-carboxamide (33). Using the general procedure for amide coupling with carboxylic acid (**15**; 80 mg, 0.22 mmol) and adamantylamine (43 mg, 0.28 mmol, 1.3 eq.) afforded the title compound (**23**; 35 mg, 32% yield). ^{1}H NMR (400MHz, DMSO-d_6) δ 8.09 - 8.05 (m, 1H), 8.04 - 7.99 (m, 1H), 7.73 (d, J = 8.8 Hz, 1H), 7.63 (d, J = 1.5 Hz, 2H), 7.45 - 7.37 (m, 2H), 3.85 (s, 3H), 2.97 (s, 3H), 2.04 (br. s., 3H), 1.99 - 1.94 (m, 6H), 1.65 (br. s., 6H). ^{13}C NMR (101MHz, DMSO-d_6) δ 164.9, 159.0, 153.9, 147.2, 144.7, 137.5, 136.3, 131.4, 129.5, 128.4, 126.7, 125.32, 125.26, 119.7, 118.4, 115.6, 56.4, 52.1, 41.2, 36.5, 21.3. EI-HR calcd for $C_{28}H_{29}ClN_5O_2$ (M^+) 502.2004, found 502.2003.

1-(2-Chloro-5-isopropoxyphenyl)-N,4-dimethyl-[1,2,4]triazolo[4,3-a]quinoxaline-8-carboxamide (34). Using the general procedure for amide coupling with carboxylic acid (**16**; 80 mg, 0.20 mmol) and 2M methylamine (131 μL, 0.26 mmol, 1.3 eq.) afforded the title compound (**34**; 61 mg, 74% yield). ^{1}H NMR (400MHz, DMSO-d_6) δ 8.62 (q, J = 4.5 Hz, 1H) 8.04 - 8.13 (m, 2 H) 7.85 (d, J = 1.5 Hz, 1 H) 7.69 (d, J = 8.6 Hz, 1 H) 7.34 - 7.40 (m, 2H) 4.70 (quin, J = 6.0 Hz, 1H) 2.96 (s, 3 H) 2.75 (d, J = 4.4 Hz, 3H) 1.29 (dd, J =16.6, 6.0 Hz, 6H). ^{13}C NMR (101MHz, DMSO-d_6) δ 165.0, 157.2, 154.1, 147.3, 144.7, 137.7, 134.6, 131.5, 129.7, 128.5, 125.8, 125.6, 124.8, 121.1, 119. 9, 115.9, 70.8, 26.9, 22.1, 22.0, 21.3. EI-HR calcd for $C_{21}H_{21}ClN_5O_2$ (M^+) 410.1378, found 410.1375.

1-(2-Chloro-5-isopropoxyphenyl)-N-isopropyl-4-methyl-[1,2,4]triazolo[4,3-a]quinoxaline-8-carboxamide (35). Using the general procedure for amide coupling with carboxylic acid (**16**; 80 mg, 0.20 mmol) and isopropylamine (23 μL, 0.26 mmol, 1.3 eq.) afforded the title compound (**35**; 30 mg, 34% yield). ^{1}H NMR (400 MHz, $CDCl_3$) δ 1H NMR (400 MHz, CDCl3) δ 8.12 (d, J = 8.4 Hz, 1H) 7.97 (dd, J = 8.4, 1.8 Hz, 1H) 7.74 (d, J = 1.7 Hz, 1H) 7.58 (d, J = 8.7 Hz, 1H) 7.22 - 7.24 (m, 1H) 7.18 - 7.22 (m, 1H) 5.52 - 5.64 (m, 1H) 4.53 - 4.67 (m, 1H) 4.17 - 4.29 (m, 1H) 3.13 (s, 3H) 1.41 (d, J = 6.1 Hz, 3H) 1.36 (d, J = 6.1 Hz, 3H) 1.23 (t, J = 6.3 Hz, 6H). ^{13}C NMR (101 MHz, $CDCl_3$) δ 164.6, 157.4, 154.5, 147.5, 144.8, 138.0, 134.7, 130.9, 130.1, 128.3, 126.0, 125.6, 125.4, 120.6, 119.4, 114.3, 71.0, 42.2, 22.8, 21.9, 21.4. EI-HR calcd for $C_{23}H_{25}ClN_5O_2$ (M^+) 438.1691, found 438.1689.

1-(2-Chloro-5-isopropoxyphenyl)-N-isobutyl-4-methyl-[1,2,4]triazolo[4,3-a]quinoxaline-8-carboxamide (36). Using the general procedure for amide coupling with carboxylic acid (**16**; 80 mg, 0.20 mmol) and isobutylamine (26 μL, 0.26 mmol, 1.3 eq.) afforded the title compound (**36**; 76 mg, 83% yield). ^{1}H NMR (400MHz, DMSO-*d*$_6$) δ 8.59 (t, J = 5.7 Hz, 1H) 8.04 - 8.16 (m, 2 H) 7.80 (d, J = 1.3 Hz, 1H) 7.68 (d, J = 8.8 Hz, 1H) 7.31 - 7.40 (m, 2H) 4.69 (spt, J = 6.0 Hz, 1H) 2.93 - 3.11 (m, 5H) 1.71 - 1.84 (m, 1H) 1.28 (dd, J = 17.6, 6.0 Hz, 6H) 0.85 (dd, J = 6.7, 1.4 Hz, 6H). ^{13}C NMR (101MHz, DMSO-*d*$_6$) δ, 165.0, 157.2, 154.0, 147.3, 144.7, 137.7, 135.1, 131.5, 129.7, 128.5, 126.0, 125.7, 124.8, 121.1, 119.8, 115.8, 70.8, 47.3, 28.5, 22.1, 22.0, 21.4, 20.6. EI-HR calcd for $C_{24}H_{27}ClN_5O_2$ (M^+) 452.1848, found 452.1847.

N-(tert-Butyl)-1-(2-chloro-5-isopropoxyphenyl)-4-methyl-[1,2,4]triazolo[4,3-a]quinoxaline-8-carboxamide (37). Using the general procedure for amide coupling with carboxylic acid (**16**;

45 mg, 0.11 mmol) and tert-butylamine (15 µL, 0.15 mmol, 1.3 eq.) afforded the title compound (**37**; 20 mg, 39% yield). ^{1}H NMR (400 MHz, MeOD-*d*$_4$) δ 8.10 (d, J = 8.3 Hz, 1H), 7.95 (dd, J = 8.6, 1.7 Hz, 1H), 7.74 - 7.58 (m, 2H), 7.37 (s, 2H), 4.72 (dt, J = 12.0, 6.1 Hz, 1H), 3.04 (s, 3H), 1.41 - 1.34 (m, 15H). ^{13}C NMR (101 MHz, MeOD-*d*$_4$) δ 166.9, 157.6, 153.7, 147.6, 144.6, 137.6, 136.5, 131.0, 129.3, 127.6, 126.1, 125.2, 120.7, 119.0, 115.0, 70.7, 51.4, 27.5, 20.79, 20.76, 19.8. EI-HR calcd for $C_{24}H_{27}ClN_5O_2$ (M^+) 452.1848, found 452.1847.

N-((3s,5s,7s)-Adamantan-1-yl)-1-(2-chloro-5-isopropoxyphenyl)-4-methyl-[1,2,4]triazolo[4,3-a]quinoxaline-8-carboxamide (38). Using the general procedure for amide coupling with carboxylic acid (**16**; 80 mg, 0.20 mmol) and adamantylamine (40 mg, 0.26 mmol, 1.3 eq.) afforded the title compound (**38**; 24 mg, 23% yield). ^{1}H NMR (400 MHz, $CDCl_3$) δ 8.10 (d, J = 8.4 Hz, 1H) 7.98 (dd, J = 8.4, 1.8 Hz, 1H) 7.61 (d, J = 1.6 Hz, 1H) 7.57 (d, J = 8.8 Hz, 1H) 7.21 - 7.23 (m, 1H) 7.17 - 7.21 (m, 1H) 5.42 (s, 1H) 4.54 - 4.66 (m, 1H) 3.11 (s, 3H) 2.15 (br. s., 3H) 1.99 - 2.05 (m, 6H) 1.71 - 1.77 (m, 6H) 1.41 (d, J = 6.0 Hz, 3H) 1.37 (d, J = 6.0 Hz, 3H). ^{13}C NMR (101 MHz, $CDCl_3$) δ 164.8, 157.4, 154.3, 147.3, 144.9, 137.8, 136.0, 131.0, 130.2, 128.5, 126.6, 125.6, 125.2, 120.6, 119.5, 113.5, 71.1, 52.6, 41.6, 36.3, 29.5, 21.9, 21.4. EI-HR calcd for $C_{30}H_{33}ClN_5O_2$ (M^+) 530.2317, found 530.2316.

1-(2-Chloro-5-isobutoxyphenyl)-N,4-dimethyl-[1,2,4]triazolo[4,3-a]quinoxaline-8-carboxamide (39). Using the general procedure for amide coupling with carboxylic acid (**17**; 80 mg, 0.19 mmol) and 2M methylamine (127 µL, 0.25 mmol, 1.3 eq.) afforded the title compound (**39**; 29 mg, 35% yield). ^{1}H NMR (400 MHz, $CDCl_3$) δ 8.05 (d, J = 8.4 Hz, 1H) 7.93 (d, J = 1.6 Hz, 1H) 7.89 (dd, J = 8.4, 1.7 Hz, 1H) 7.56 (d, J = 8.9 Hz, 1H) 7.15 - 7.23 (m, 2H) 6.36 (d, J =

4.5 Hz, 1H) 3.70 - 3.83 (m, 2H) 3.09 (s, 3H) 2.97 (d, J = 4.8 Hz, 3H) 2.01 - 2.19 (m, 1H) 1.02 (dd, J = 6.7, 0.6 Hz, 6H). ^{13}C NMR (101 MHz, $CDCl_3$) δ 166.0, 158.6, 154.5, 147.8, 144.8, 138.0, 134.2, 130.9, 129.9, 127.9, 125.6, 125.6, 125.2, 119.6, 118.1, 115.4, 75.1, 28.2, 27.1, 21.4, 19.2. EI-HR calcd for $C_{22}H_{23}ClN_5O_2$ (M^+) 424.1535, found 424.1532.

1-(2-Chloro-5-isobutoxyphenyl)-N-isopropyl-4-methyl-[1,2,4]triazolo[4,3-a]quinoxaline-8-carboxamide (40). Using the general procedure for amide coupling with carboxylic acid (**17**; 80 mg, 0.19 mmol) and isopropylamine (22 μL, 0.25 mmol, 1.3 eq.) afforded the title compound (**40**; 30 mg, 34% yield). ^{1}H NMR (400 MHz, $CDCl_3$) δ 8.06 (d, J = 8.4 Hz, 1H) 7.94 (dd, J = 8.4, 1.7 Hz, 1H) 7.75 (d, J = 1.6 Hz, 1H) 7.55 (d, J = 8.7 Hz, 1H) 7.22 - 7.24 (m, 1H) 7.16 - 7.21 (m, 1H) 5.78 (d, J = 7.7 Hz, 1H) 4.13 - 4.25 (m, 1H) 3.71 - 3.82 (m, 2H) 3.09 (s, 3H) 2.04 - 2.16 (m, 1H) 1.18 - 1.23 (m, 6H) 1.02 (d, J = 6.7 Hz, 6H). ^{13}C NMR (101 MHz, $CDCl_3$) δ 164.6, 158.6, 154.4, 147.5, 144.8, 137.9, 134.7, 130.8, 130.0, 128.2, 125.9, 125.6, 125.4, 119.6, 118.2, 114.5, 75.1, 42.2, 28.2, 22. 8, 21.4, 19.1. EI-HR calcd for $C_{24}H_{27}ClN_5O_2$ (M^+) 452.1848, found 452.1847.

1-(2-Chloro-5-isobutoxyphenyl)-N-isobutyl-4-methyl-[1,2,4]triazolo[4,3-a]quinoxaline-8-carboxamide (41). Using the general procedure for amide coupling with carboxylic acid (**17**; 80 mg, 0.19 mmol) and isobutylamine (25 μL, 0.25 mmol, 1.3 eq.) afforded the title compound (**41**; 29 mg, 32% yield). ^{1}H NMR (400 MHz, $CDCl_3$) δ 8.09 (d, J = 8.4 Hz, 1H) 7.96 (dd, J = 8.4, 1.8 Hz, 1H) 7.81 (d, J = 1.6 Hz, 1H) 7.54 (d, J = 8.8 Hz, 1H) 7.23 (d, J = 2.9 Hz, 1H) 7.19 (dd, J = 8.9, 3.0 Hz, 1H) 6.03 (t, J = 5.3 Hz, 1H) 3.70 - 3.83 (m, 2H) 3.17 - 3.29 (m, 2H) 3.10 (s, 3H) 2.04 - 2.18 (m, 1H) 1.79 - 1.87 (m, 1H) 1.03 (d, J = 6.6 Hz, 6H) 0.95 (dd, J = 6.7, 1.8 Hz, 6H).

^{13}C NMR (101 MHz, $CDCl_3$) δ 165.6, 158.6, 154.5, 147.6, 144.8, 138.0, 134.6, 130.8, 130.1, 128.1, 125.9, 125.6, 125.5, 119.6, 118.2, 114.4, 75.1, 47.5, 28.5, 28.2, 21.4, 20.2, 19.2. EI-HR calcd for $C_{25}H_{29}ClN_5O_2$ (M^+) 466.2004, found 466.2000.

N-(tert-Butyl)-1-(2-chloro-5-isobutoxyphenyl)-4-methyl-[1,2,4]triazolo[4,3-a]quinoxaline-8-carboxamide (42). Using the general procedure for amide coupling with carboxylic acid (**17**; 80 mg, 0.19 mmol) and tert-butylamine (27 μL, 0.25 mmol, 1.3 eq.) afforded the title compound (42; 51 mg, 57% yield). ^{1}H NMR (400 MHz, $CDCl_3$) δ 8.10 (d, J = 8.4 Hz, 1H) 7.98 (dd, J = 8.4, 1.8 Hz, 1H) 7.62 (d, J = 1.6 Hz, 1H) 7.56 (d, J = 8.8 Hz, 1H) 7.24 - 7.26 (m, 1H) 7.19 - 7.23 (m, 1H) 5.59 (s, 1H) 3.71 - 3.84 (m, 2H) 3.11 (s, 3H) 2.07 - 2.19 (m, 1H) 1.41 (s, 9H) 1.04 (d, J = 6.7 Hz, 6H). ^{13}C NMR (101 MHz, $CDCl_3$) δ 165.0, 158.7, 154.3, 147.4, 144.8, 137.8, 135.9, 130.8, 130.2, 128.4, 126.5, 125.7, 125.2, 119.6, 118.2, 113.6, 75.2, 51.9, 28.8, 28.2, 21.4, 19.1. EI-HR calcd for $C_{25}H_{29}ClN_5O_2$ (M^+) 466.2004, found 466.2004.

N-((3s,5s,7s)-Adamantan-1-yl)-1-(2-chloro-5-isobutoxyphenyl)-4-methyl-[1,2,4]triazolo[4,3-a]quinoxaline-8-carboxamide (43). Using the general procedure for amide coupling reaction with carboxylic acid (**17**; 80 mg, 0.19 mmol) and adamantylamine (38 mg, 0.25 mmol, 1.3 eq.) afforded the title compound (**43**; 43 mg, 41% yield). ^{1}H NMR (400 MHz, $CDCl_3$) δ 8.08 (d, J = 8.4 Hz, 1H) 7.97 (dd, J = 8.4, 1.8 Hz, 1H) 7.61 (d, J = 1.6 Hz, 1H) 7.57 (d, J = 8.8 Hz, 1H) 7.26 - 7.23 (m, 1H) 7.23 - 7.18 (m, 1H) 5.43 (s, 1H) 3.72 - 3.84 (m, 2H) 3.10 (s, 3H) 2.17 - 2.12 (m, 3H) 2.12 - 2.07 (m, 1H) 2.02 (d, J = 2.4 Hz, 6H) 1.76 - 1.70 (m, 6H) 1.04 (d, J = 6.7 Hz, 6H). ^{13}C NMR (101 MHz, $CDCl_3$) δ 164.8, 158.6, 154.3, 147.3, 144.8, 137.8, 136.0, 130.9, 130.2,

128.4, 126.5, 125.7, 125.2, 119.6, 118.2, 113.6, 75.2, 52.6, 41.6, 36.3, 29.4, 28.2, 21.4, 19.1. EI-HR calcd for $C_{31}H_{35}ClN_5O_2$ (M^+) 544.2474, found 544.2470.

1-(5-(tert-Butoxy)-2-chlorophenyl)-N,4-dimethyl-[1,2,4]triazolo[4,3-a]quinoxaline-8-carboxamide (44). Using the general procedure for amide coupling with carboxylic acid (**18**; 45 mg, 0.11 mmol) and 2.0 M methylamine (70 μL, 0.14 mmol, 1.3 eq.) afforded the title compound (**44**; 24 mg, 52% yield). ^{1}H NMR (400 MHz, MeOD-*d*$_4$) δ 8.10 (d, J = 8.6 Hz, 1H), 7.99 (dd, J = 8.6, 1.7 Hz, 1H), 7.90 (d, J = 1.7 Hz, 1H), 7.67 (d, J = 8.6 Hz, 1H), 7.45 - 7.37 (m, 2H), 3.05 (s, 3H), 2.88 (s, 3H), 1.42 (s, 9H). ^{13}C NMR (101 MHz, MeOD-*d*$_4$) δ 166.7, 155.3, 154.0, 147.5, 144.6, 137.8, 134.63, 130.8, 129.4, 128.6, 128.5, 127.2, 127.0, 125.5, 125.3, 115.6, 80.0, 27.9, 25.9, 20.0. EI-HR calcd for $C_{22}H_{23}ClN_5O_2$ (M^+) 424.1535, found 424.1535.

1-(5-(tert-Butoxy)-2-chlorophenyl)-N-isopropyl-4-methyl-[1,2,4]triazolo[4,3-a]quinoxaline-8-carboxamide (45). Using the general procedure for amide coupling with carboxylic acid (**18**; 45 mg, 0.11 mmol) and isopropylamine (8.4 mg, 0.14 mmol, 1.3 eq.) afforded the title compound (**18**; 25 mg, 51% yield). ^{1}H NMR (400 MHz, MeOD-*d*$_4$) δ 8.15 - 8.06 (m, 1H), 8.05 – 7.97 (m, 1H), 7.82 (d, J = 1.7 Hz, 1H), 7.76 - 7.63 (m, 1H), 7.50 - 7.37 (m, 2H), 4.11 (dt, J = 13.2, 6.6 Hz, 1H), 3.04 (s, 3H), 1.42 (s, 9H),1.22 (dd, J = 9.8, 6.6 Hz, 6H). ^{13}C NMR (101 MHz, MeOD-*d*$_4$) δ 165.7, 155.4, 153.9, 147.4, 144.6, 137.8, 135.1, 130.7, 129.3, 128.5, 128.4, 127.3, 127.1, 125.6, 125.4,115.5, 79.9, 42.0, 27.7, 21.2, 21.1,19.8. EI-HR calcd for $C_{24}H_{27}ClN_5O_2$ (M^+) 452.1848, found 452.1850.

1-(5-(tert-Butoxy)-2-chlorophenyl)-N-isobutyl-4-methyl-[1,2,4]triazolo[4,3-a]quinoxaline-8-carboxamide (46). Using the general procedure for amide coupling with carboxylic acid (**18**; 10 mg, 0.024 mmol) and isobutylamine (2.3 mg, 0.032 mmol, 1.3 eq.) afforded the title compound (**46**; 7 mg, 57% yield). ^{1}H NMR (400 MHz, MeOD-d_4) δ 8.13 (d, J = 8.3 Hz, 1H), 8.02 (dd, J = 8.4, 1.8 Hz, 1H), 7.86 (d, J = 1.7 Hz, 1H), 7.71 - 7.65 (m, 1H), 7.45 - 7.39 (m, 2H), 3.23 - 3.06 (m, 2H), 3.05 (s, 3H), 1.87 (dt, J = 13.6, 6.8 Hz, 1H), 1.42 (s, 9H), 0.95 (dd, J = 6.7, 0.9 Hz, 6H). ^{13}C NMR (101 MHz, MeOD-d_4) δ 166.6, 155.38, 154.0,147.4, 144.6,137.8, 135.1, 130.7, 129.4, 128.5, 128.4, 127.2, 127.1, 125.5, 115.4, 79.9, 28.4, 27.7, 19.8, 19.22, 19.19. EI-HR calcd for $C_{25}H_{29}ClN_5O_2$ (M^+) 466.2004, found 466.2002.

1-(5-(tert-Butoxy)-2-chlorophenyl)-N-(tert-butyl)-4-methyl-[1,2,4]triazolo[4,3-a]quinoxaline-8-carboxamide (47). Using the general procedure for amide coupling with carboxylic acid (**18**; 30 mg, 0.073 mmol) and tert-butylamine (10.0 µL, 0.095 mmol, 1.3 eq.) afforded the title compound (**47**; 16 mg, 47% yield). ^{1}H NMR (400 MHz, MeOD-d_4) δ 8.09 (d, J = 8.3 Hz, 1H), 8.0 (dd, J = 8.3,1.7 Hz, 1H), 7.74 - 7.63 (m, 3H), 7.48 - 7.42 (m, 2H), 3.04 (s, 3H), 1.43 (s, 9H) 1.40 (s, 9H). ^{13}C NMR (101 MHz, MeOD-d_4) δ 166.6, 155.4, 153.8, 147.3, 144.6, 137.6, 136.5, 130.7, 129.3, 128.5, 127.3, 127.1, 126.0, 125.2, 115.0, 79.9, 51.4, 27.7, 27.5, 19.8. EI-HR calcd for $C_{25}H_{29}ClN_5O_2$ (M^+) 466.2004, found 466.2003.

N-((3s,5s,7s)-Adamantan-1-yl)-1-(5-(tert-butoxy)-2-chlorophenyl)-4-methyl-[1,2,4]triazolo[4,3-a]quinoxaline-8-carboxamide (48). Using the general procedure for amide coupling with carboxylic acid (**18**; 42 mg, 0.10 mmol) and adamantylamine (20 mg, 0.13 mmol, 1.3 eq.) afforded the title compound (**48**; 15 mg, 27% yield). ^{1}H NMR (400 MHz, MeOD-d_4) δ

ppm 1.43 (s, 9 H) 1.72 - 1.82 (m, 6 H) 2.03 - 2.16 (m, 9 H) 3.05 (s, 3 H) 7.38 (s, 0.5 H) 7.39 - 7.48 (m, 2 H) 7.67 (d, J = 1.7 Hz, 1 H) 7.70 (d, J = 8.8 Hz, 1 H) 7.84 - 7.87 (m, 0.5 H) 7.95 (dd, J = 8.6, 1.7 Hz, 1 H) 8.10 (d, J = 8.3 Hz, 1 H) ^{13}C NMR (101 MHz, MeOD-d_4) δ 166.3, 155.3, 153.7, 147.3, 144.6, 137.6, 136.6, 130.8, 129.4, 128.6, 128.4, 127.3, 127.1, 126.1, 125.1, 114.9, 80.0, 52.4, 40.9, 36.1, 29.5, 29.4, 27.9, 20.0. EI-HR calcd for $C_{31}H_{35}ClN_5O_2$ (M^+) 544.2474, found 544.2470.

PDE2 crystallography. Crystal structures of PDE2 ligand co-complexes were determined following previously described methods.[15] The catalytic domain of PDE2 (residues 579-918) was overexpressed in baculovirus insect cells and purified through affinity and size-exclusion chromatography. Crystals were obtained in the presence of 2mM of 3-isobutyl-1-methylxanthine (IBMX) which was added to the well solution containing 17-19% PEG3350, 0.2M MgCl2, 0.1M Tris, pH 8.4. Crystals were then soaked overnight in reservoir buffer containing 1mM of target compound and flash frozen in liquid nitrogen in the presence of 25% glycerol used as a cryoprotectant. The diffraction data sets were collected at the Advanced Light Source beamline 5.0.1 and processed with DIALS[18] or HKL2000.[19] The structures were solved by molecular replacement using Phaser[20], model building using COOT[21] and refinement using PHENIX.[22] The structure of compound 43 shows a highly disordered adamantyl group in the R^1 solvent-exposed pocket and therefore the occupancy of the adamantyl group was set to zero during refinement. Data collection and refinement statistics are summarized in the supplemental information. Figures representing the crystal structures were generated with PyMOL (The PyMOL Molecular Graphics System, Version 1.7.6.4 Schrödinger, LLC).

PDE Inhibition. PDE2 inhibition IC_{50} values were determined by an IMAP assay measuring inhibition of FAM-cAMP hydrolysis by full length PDE2 enzymes. Specifically, in 1536 well white plates, 250 pg per well GST tagged PDE2 was dispensed in 2.5 μL IMAP assay buffer consisting of 10 mM Tris pH 7.2, 10 mM $MgCl_2$, 1 mM DTT, 0.1 % fatty acid free BSA, with 10 U/ml calmodulin, and 2.5 mM $CaCl_2$. 30 nl compound was then added from 1 mM stock in DMSO using the Kalypsys 1536 pintool. Plates were incubated for 5 minutes at rt before dispensing 1.5 μL of 533 nM FAM-cAMP for a final concentration of 200 nM. The plates were incubated 30 minutes at rt after a brief centrifugation. The assay was terminated by adding 5 μL IMAP binding reagent Tb complex to each well, prepared according to manufacturer's recommendations. Plates were incubated 1 hour at rt and read on a Viewlux multimode plate reader (Perkin Elmer).

ASSOCIATED CONTENT

Supporting Information. Activity data for all compounds in the matrix, computational details (lowest energy conformation, tSA calculation, RMSD and non-additivity values), protein crystallographic data statistics tables, molecular formula strings.

PDB ID Codes. Crystal structures of PDE2 in complex with **19, 23, 31, 39, 43, 46** have been deposited in the RCSB RCSB Protein Data Bank under the accession codes of 6C7E, 6C7D, 6C7I, 6C7F, 6C7G, 6C7J, respectively.

AUTHOR INFORMATION

Corresponding Author

* E-mail: gomezlaurent0@gmail.com

ACKNOWLEDGMENT

The Advanced Light Source is supported by the Director, Office of Science, Office of Basic Energy Sciences, of the U.S. Department of Energy under Contract No. DE-AC02-05CH11231.

ABBREVIATIONS USED

SAR, structure-activity-relationship; QSAR, quantitative structure–activity relationship; MW, molecular weight; tPSA, topological polar surface area; FEP, free energy perturbation; PDE2, phosphodiesterase 2; RMSD, root-mean-square deviation; cLogP, calculated partition coefficient;

REFERENCES

(1) Free, S.M.; Wilson, J.W. A mathematical contribution to structure-activity studies. *J. Med. Chem.*, **1964**, *7*, 395-399.

(2) Cammareta, A. Interrelationship of the regression models used for structure-activity analyses. *J. Med. Chem.*, **1972**, *15*, 573-577.

(3) Jencks, W.P. On the attribution and additivity of binding energies. *Proc. Natl. Acad. Sci. U.S.A*. **1981**, *78*, 4046-4050.

(4) Patel, Y.; Gillet, V.J.; Howe, T.; Pastor, J.; Oyarzabal, J.; Willett, P. Assessment of additive/nonadditive effects in structure-activity relationships: implications for iterative drug design. *J. Med. Chem.,* **2008**, *51*, 7552-7562.

(5) Wang, L., Wu, Y., Deng, Y., Kim., B., Pierce, L., Krilov, G., Lupyan,, D., Robinson, S., Dahlgren, M., Greenwood, J., Romero, D. L., Masse, C., Knight, J. L., Steinbrecher, T., Beuning, T., Damm, W., Harder, E., Sherman, W., Brewer, M., Wesler, R., Murcko, M., Frye, L., Farid, R., Lin, T., Mobley, D. L., Jorgensen, W. L., Berne, B. J., Friesner, R. A., Abel, R. Accurate and reliable prediction of relative ligand binding potency in prospective drug discovery by way of a

modern free-energy calculation protocol and force field., *J. Am. Chem. Soc*., **2015**, *137*, 2695-2703.

(6) https://drugdesigndata.org/ accessed on June 8th 2017.

(7) (a) D. Mobeley, M. K. Gilson. Predicting binding free energies: frontiers and benchmarks. Annu. Rev. Biophys., 2017, 46, 531-58. (b) Dimova, D., Bajorath, J. Advances in activity cliff research. *Mol. Inform*., **2016**, *35*, 181-191.

(8) McClure, K.; Hack, M.; Huang, L.; Sehon, C.; Morton, M.; Barrett, T.; Shankley, N.; Breitenbucher, J.G. Pyrazole CCK(1) receptor antagonists. Part 1: solution-phase library synthesis and determination of Free-Wilson additivity. *Bioorg. Med. Chem. Lett*., **2006**, *16*, 72-76.

(9) Sehon, C.; McClure, K.; Hack, M.; Morton, M.; Gomez, L.; Li, L.; Barrett, T. D.; Shankley, N,; Breitenbucher, J.G. Pyrazole CCK(1) receptor antagonists. Part 2: SAR studies by solid-phase library synthesis and determination of Free-Wilson additivity. *Bioorg. Med. Chem. Lett*., **2006**, *16*, 77-80.

(10) Baum, B.; Muley, L.; Smolinski M.;Heine, A.; Hangauer, D.; Klebe, G. Non-additivity of functional group contributions in protein-ligand binding: a comprehensive study by crystallography and isothermal titration calorimetry. *J. Mol. Biol*., **2010**, *397*, 1042–1054.

(11) Schauperl, M., Czodrowski, P., Fuchs, E. J., Huber, R. G., Waldner, B. J., Podewitz, M., Kramer, C., Liedl, K. R. Binding pose flip explained via enthalpic and entropic contributions. *J. Chem. Inf. Model.*, **2017**, *57*, 345-354.

(12) Schiebel, J., Gapspari, R., Sandner, A., Ngo, K., Gerber, H.J., Cavalli, A., Ostermann, A., Heine, A., Klebe, G. Charges shift protonation: neutron diffraction reveals that aniline and 2-aminopyridine become protonated upon binding to trypsin. *Angewandte Chemie, Int. Ed.*, **2017**, *56*, 4887-4890.

(13) Kramer, C.; Fuchs, J. E.; Liedl, K. R. Strong nonadditivity as a key structure-activity relationship feature: distinguishing structural changes from assay artifacts. *J. Chem. Inf. Model*., **2015**, *55*, 483-494.

(14) Andres-Gil, J. I.; Rombouts, F. J. R.; Trabanco-Suarez, A. A.; Vanhoof, G. C. P.; Buijnsters, A.; Guillemont, J. E. G.; Bormans, G. M. R.; Celen, S. J. L.; Vliegen, M. Preparation of (Un)labeled 1-aryl-4-methyl-[1,2,4]triazolo[4,3-a]quinoxaline Derivatives as PDE2 and PDE10 Inhibitors for Therapy and Imaging. WO2013000924 (2013).

(15) a) Zhu, J.; Yang, Q.; Dai, D.; Huang, Q. X-ray crystal structure of phosphodiesterase 2 in complex with a highly selective, nanomolar inhibitor reveals a binding-induced pocket important for selectivity. *J. Am. Chem. Soc*. **2013**, *135*, 11708-11711; b) Pérez-Benito, L.; Keränen, H.; van Vlijmen, H.; Tresadern, G. Predicting binding free energies of PDE2 inhibitors. The difficulties of protein conformation. *Scientific Reports*, **2018**, *8:* 4883.

(16) a) Najmanovich, R.; Kuttner, J.; Sobolev, V.; Edelman, M. Side-chain flexibility in proteins upon ligand binding. *Protein*, **2000**, *39*, 261-268. b) Teague, S. J. Implications of protein flexibility for drug discovery. Nature review: drug discovery 2:527-541, 2003.

(17) a) Gianni, S.; Dogan, J.; Jemth, P. Distinguishing induced fit from conformational selection. Biophysical Chemistry, 189: 33-39, 2014. b) Vogt, A.D.; Pozzi, N.; Chen, Z.; Di Cera, E. Essential role of conformational selection in ligand binding. *Biophys. Chem*., **2014**, *186*, 13-21.

(18) Watermana, D.G.; Winterb, G.; Parkhurstb, J.M.; Fuentes-Monterob, L.; Hattnec, J.; Brewsterc, A.; Sauterc, N.K.; Evans, G. The DIALS framework for integration software. *CCP4 Newsl. Protein Crystallogr.* **2013**, *49*, 16–19.

(19) Otwinowski, Z.; Minor, W. Processing of X-ray diffraction data collected in oscillation mode, *Methods in Enzymology: Macromolecular Crystallography*, *part A*, **1997**, *276*, 307-326, C.W. Carter, Jr. & R. M. Sweet, Eds., Academic Press (New York).

(20) McCoy, A.J.; Grosse-Kunstleve, R.W.; Adams, P.D.; Winn, M.D.; Storoni, L.C.; Read, R.J. Phaser crystallographic software. *J. Appl. Cryst*. **2007**, *40*, 658-674.

(21) Emsley, P.; Lohkamp, B.; Scott, W.G.; Cowtan, K. Features and development of Coot. *Acta Crystallogr D Biol Crystallogr.* **2010**, *66*, 486-501.

(22) Afonine, P.V.; Grosse-Kunstleve, R.W.; Echols, N.; Headd, J.J.; Moriarty, N.W.; Mustyakimov, M.; Terwilliger, T.C.; Urzhumtsev, A.; Zwart, P.H.; Adams, P.D. Towards automated crystallographic structure refinement with phenix.refine. *Acta Crystallogr., Sect. D: Biol. Crystallogr.* **2012**, 68, 352-367.

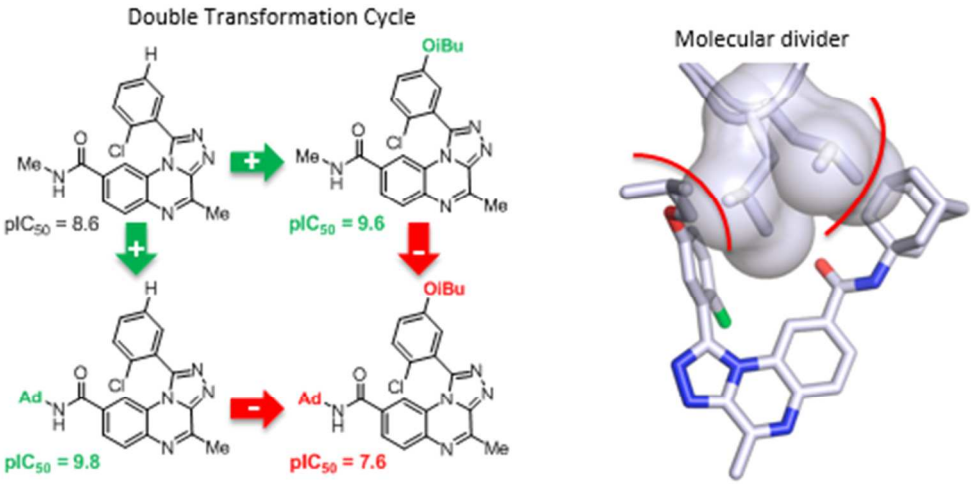

Table of Contents graphic